JOURNAL OF GEOPHYSICAL RESEARCH, VOL. 112, D19302, doi:10.1029/2006JD007403, 2007

Modeling the photochemical origins of the extreme deuterium enrichment in stratospheric H_2

Kathleen A. Mar,[1] Michael C. McCarthy,[2] Peter Connell,[3] and Kristie A. Boering[1,4]

Received 13 April 2006; revised 16 May 2007; accepted 21 June 2007; published 4 October 2007.

[1] The isotopic composition of H_2 produced by methane oxidation ("$\delta D_{h\nu}$") is an important yet poorly constrained term in the global H_2 isotope budget. Box model analyses of the extreme deuterium enrichment in stratospheric H_2 demonstrated empirically that $\delta D_{h\nu}$ is much larger than the initial δD of CH_4, a conclusion that qualitatively resolved major discrepancies between the global H_2 concentration and isotope budgets. However, the box model studies necessarily assumed that the isotopic fractionation factor for the conversion of CH_4 to H_2 remains constant throughout the stratosphere and that $\delta D_{h\nu}$ for the troposphere is equal to, or can be easily extrapolated from, the stratospheric value. Here, we use a 2-D chemical-radiative-transport model to investigate these assumptions by determining the sensitivity of the isotopic composition of H_2 (δD-H_2) and $\delta D_{h\nu}$ to known and unknown isotope effects in the elementary steps of the photochemical production and destruction of H_2. Our results show that four categories of isotopic fractionation, (1) kinetic isotope effects (KIEs) for CH_4 and H_2 oxidation, (2) H versus D abstraction for CH_3D oxidation to H_2 or HD, (3) KIEs for CH_2O oxidation, and (4) isotope effects for CH_2O photolysis, all play significant but varying roles in determining δD-H_2 and $\delta D_{h\nu}$ in the stratosphere and troposphere. Furthermore, we show that calculated $\delta D_{h\nu}$ values vary significantly with latitude and altitude, leading to larger uncertainties in $\delta D_{h\nu}$ than previously estimated. Using these sensitivities, we also identify the laboratory experiments, theoretical calculations, and observations most needed to reduce uncertainties in the magnitude of $\delta D_{h\nu}$ and, hence, the global H_2 isotope budget.

Citation: Mar, K. A., M. C. McCarthy, P. Connell, and K. A. Boering (2007), Modeling the photochemical origins of the extreme deuterium enrichment in stratospheric H_2, *J. Geophys. Res.*, *112*, D19302, doi:10.1029/2006JD007403.

1. Introduction

[2] Hydrogen fuel cells produce energy from the controlled oxidation of molecular hydrogen (H_2) and have been proposed as an alternative to direct fossil fuel combustion. However, a shift to hydrogen fuel cell technologies would likely increase anthropogenic H_2 emissions due to leakage from the requisite infrastructure. If such emissions were to result in significant increases in the atmospheric H_2 burden, some studies have predicted a reduction in stratospheric ozone due to increases in stratospheric water vapor from H_2 oxidation and changes in microbial communities in natural soils that are host to microorganisms that metabolize H_2 [*Tromp et al.*, 2003; *Warwick et al.*, 2004]. Furthermore, regional air quality, the oxidation capacity of the troposphere, and radiative forcing might be affected as additional H_2 reacts with OH radicals [*Prather*, 2003; *Schultz et al.*, 2003; *Warwick et al.*, 2004]. The magnitudes of these potential effects, however, are largely uncertain, because of uncertainties in possible leakage rates and in the magnitudes of the current H_2 sources and sinks and how they may change over time. Thus, in order to accurately predict the response of the biosphere-atmosphere system to any future increases in anthropogenic H_2 emissions, a quantitative understanding of the current H_2 budget is required.

[3] Estimates of the magnitudes of the H_2 sources (e.g., fossil fuel burning, biomass burning, oxidation of methane and nonmethane hydrocarbons) and H_2 sinks (e.g., reaction with OH radicals, uptake by soils followed by microbial degradation) based on atmospheric H_2 concentration measurements around the globe have large uncertainties, ranging from ±30 to ±70% [*Hauglustaine and Ehhalt*, 2002; *Novelli et al.*, 1999]; see Table 1. Because many of the various sources and sinks of H_2 have or impart distinct deuterium isotopic signatures (Table 1), the deuterium content of atmospheric H_2 can serve as an additional constraint on H_2 budget estimates [e.g., *Gerst and Quay*, 2001; *Rhee et al.*, 2006a]. However, until recently, the global H_2 and isotope budgets were in apparent disagreement: analyses of H_2 concentration measurements suggested that uptake by soils was the largest sink [e.g., *Hauglustaine and Ehhalt*,

[1]Department of Chemistry, University of California, Berkeley, California, USA.
[2]Sonoma Technology, Inc., Petaluma, California, USA.
[3]Energy and Environment Directorate, Lawrence Livermore National Laboratory, Livermore, California, USA.
[4]Also at Department of Earth and Planetary Science, University of California, Berkeley, California, USA.

0148-0227/07/2006JD007403$09.00

Table 1. Hydrogen Budget Estimates From H_2 Concentration Constraints and the Isotopic Composition and KIEs for H_2 Sources and Sinks

Sources	*Novelli et al.* [1999], Tg yr^{-1}	*Hauglustaine and Ehhalt* [2002], Tg yr^{-1}	δD (‰ VSMOW)[a]	References for δD
Fossil fuel combustion	15 ± 10	16	−196 ± 10	*Gerst and Quay* [2001]
Biomass burning	16 ± 9	13	−290 ± 60	*Gerst and Quay* [2001]
CH_4 oxidation	26 ± 9	31[b]	+190 ± 50[c]	*Rhee et al.* [2006b]
			+310 ± 50[d]	*Rhee et al.* [2006b]
			+180 ± 50[d]	*Röckmann et al.* [2003]
			+213[c,d,e]	*Rahn et al.* [2003]
			+130 ± 70[b,f]	*Gerst and Quay* [2001]
NMHC oxidation	14 ± 7			
Biogenic N_2 fixation	3 ± 1	5	−700	*Rahn et al.* [2003]
Oceans	3 ± 2	5	−700	*Rahn et al.* [2003]
Total sources	77 ± 16	70		
Sinks	***Novelli et al.* [1999], Tg yr^{-1}**	***Hauglustaine and Ehhalt* [2002], Tg yr^{-1}**	**KIE (k_H/k_D)[g]**	**References for KIE**
OH oxidation of H_2	19 ± 5	15	1.08exp(130 ± 25/T)	*Talukdar et al.* [1996]
			1.65 ± 0.05	*Ehhalt et al.* [1989]
Soil uptake	56 ± 41	55	1.06 ± 0.024	*Gerst and Quay* [2001]
Total sinks	75 ± 41	70		

[a] $\delta D = ((D/H)_{sample}/(D/H)_{standard} - 1) \times 1000$, the isotopic composition of a species in delta notation.
[b] NMHC oxidation source included with CH_4 oxidation.
[c] For the troposphere with $\delta D-CH_4 = -90‰$.
[d] For the stratosphere with $\delta D-CH_4 = -80$, -90, and $-86‰$ for *Rhee et al.* [2006b], *Röckmann et al.* [2003], and *Rahn et al.* [2003], respectively.
[e] See section 1 for a discussion of uncertainty.
[f] From tropospheric budget arguments. Includes N_2 fixation and ocean source terms.
[g] k_H/k_D = the ratio of the rate coefficients for loss of H_2 versus loss of HD.

2002] while those of the hydrogen isotopic composition suggested that reaction with OH was the major sink [*Ehhalt et al.*, 1989]. Recent observations and box model analyses of the extreme deuterium enrichment in stratospheric H_2 resolved this major discrepancy by showing empirically that methane oxidation (see Figure 1) results in H_2 that is significantly more enriched in deuterium than the reactant methane [*Rahn et al.*, 2003; *Röckmann et al.*, 2003], as first hypothesized by *Gerst and Quay* [2001] from tropospheric budget arguments. Both stratospheric studies used box models to estimate values for the isotopic composition of H_2 produced by methane oxidation (or "$\delta D_{h\nu}$," see equation (5)) near the tropopause of ∼215‰ [*Rahn et al.*, 2003] and 180 ± 50‰ [*Röckmann et al.*, 2003], values isotopically heavy enough to counterbalance the isotopically light sources from, e.g., fossil fuel and biomass burning and to reconcile the isotope and concentration budgets if such dramatic deuterium enrichment in the overall $CH_4 \rightarrow H_2$ oxidation pathway is also valid for the troposphere.

[4] Significant uncertainties, however, remain. The box model analyses noted above necessarily assumed that a single value for the isotopic fractionation factor describing the change in the D/H ratio from the reactant CH_4 to the product H_2 (or "$\alpha_{CH4\rightarrow H2}$") was valid for the entire stratosphere and that oxidant concentrations and mixing ratios, temperature-dependent reaction rate coefficients, and the yield of H_2 for each CH_4 molecule lost were constant. *Rahn et al.* [2003] estimated that the uncertainties associated with these assumptions alone (specifically, that conditions at an altitude of 30 km in the tropics applied to the entire stratosphere) might lead to a range of possible values for $\delta D_{h\nu}$ of 450‰ (based on the uncertainty range given for $\alpha_{CH4\rightarrow H2} = 1.33$ of (+0.29, −0.25)), while only conceptual arguments were given that similar magnitudes for $\alpha_{CH4\rightarrow H2}$ might be found in the troposphere. *Röckmann et al.* [2003] gave estimates for $\delta D_{h\nu}$ for the stratosphere and tropopause only, while recently *Rhee et al.* [2006b] used a more sophisticated box model using averaged output from a 2-D model to reexamine their stratospheric observations (yielding quite different results for stratospheric $\delta D_{h\nu}$ from their earlier estimate) and to extrapolate the stratospheric results to the troposphere (see Table 1). In this study, we use LOTUS, the Lawrence Livermore National Laboratory (LLNL) 2-D model of the atmosphere, to investigate directly the sensitivities of the isotopic composition of stratospheric H_2 (i.e., δD-H_2), $\alpha_{CH4\rightarrow H2}$, and $\delta D_{h\nu}$ to spatial and temporal variations in chemistry, radiation, and mass transport which occur throughout the stratosphere and troposphere not possible using box models. To do so, isotope effects for all the individual reaction steps from CH_4 to H_2 (Figure 1) are included since the rates of many of these individual steps are known to be or are likely to be sensitive to temperature, radiation, and/or oxidant concentration differences in different regions of the atmosphere. Several of these isotope effects are not known, however, and, as we will show, are not constrained by the combination of stratospheric and surface observations and laboratory measurements that are currently available. Furthermore, depending on their characteristics and magnitudes, these isotope effects may result in considerable differences between stratospheric and tropospheric values for $\delta D_{h\nu}$ and differences which may be difficult to predict with box models alone. Thus we note that a main objective of our study is not to derive more accurate or precise estimates for $\delta D_{h\nu}$ for use in global isotope budgets but (1) to investigate the extent to which current uncertainties in these isotope effects may limit the accuracy and precision of estimates of $\delta D_{h\nu}$ and (2) to use the modeling results to prioritize the laboratory experiments, theoretical calculations, and atmo-

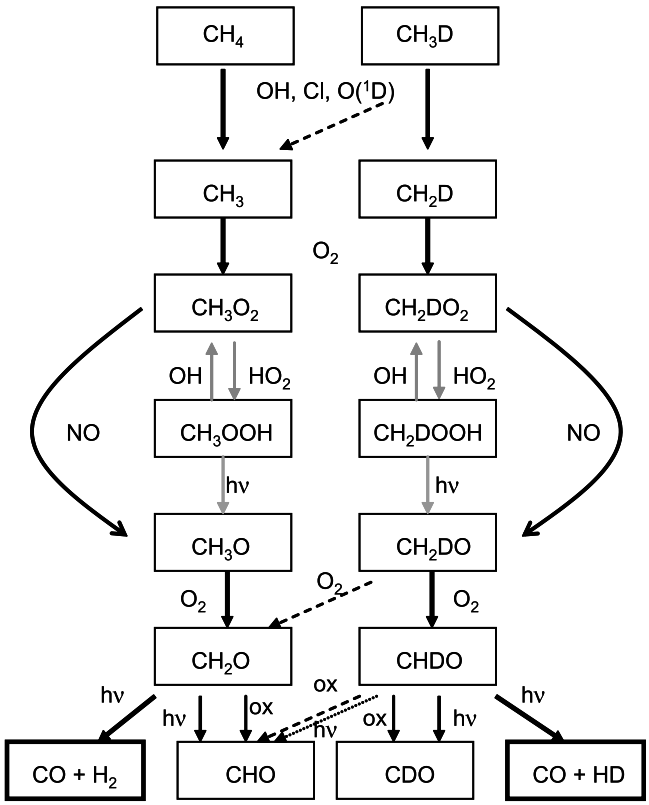

Figure 1. Simplified schematic diagram of the reaction pathway from methane to molecular hydrogen, modified from *Rahn et al.* [2003]. Reactions with multiple pathways have relative magnitudes represented by arrow thickness, and "ox" is an abbreviation for oxidants (for a list of specific oxidants, see Table 2). Steps with gray shading are examples of reactions that are important in the troposphere but are less significant in the stratosphere. Atom abstraction reactions that remove D during the oxidation sequence do so irreversibly with respect to formation of HD and are represented by arrows crossing the center to the left.

spheric observations needed to significantly reduce uncertainties in the global H_2 isotope budget.

2. Isotope-Specific Chemistry in the LLNL 2-D Model and Model Scenarios

[5] Isotope-specific reactions of CH_4, H_2, and their oxidation intermediates were modeled using LOTUS, the LLNL two-dimensional chemical-radiative-transport model. The model calculates zonal average distributions of chemically active trace constituents in the troposphere and stratosphere and has been used in ozone assessment studies [e.g., *Kinnison et al.*, 1994; *World Meteorological Organization*, 1999] as well as in studies of the isotopic composition of methane [*McCarthy et al.*, 2001, 2003] in which we used model calculations and observations of δD-CH_4 and δ^{13}C-CH_4 to constrain the magnitudes of several KIEs. The processes represented in LOTUS include (1) thermal kinetic chemical reactions with rate coefficients based on climatological zonal temperature distributions; (2) photolytic chemical reactions; (3) advection and diffusion driven by climatological zonal average temperature, radiative transfer of energy, and orographic forcing; (4) surface emission and in situ production of active trace constituents; and (5) removal of active species by dry and wet deposition. The model domain extends from pole to pole and from the surface to 85 km. The horizontal resolution is 5° in latitude and the vertical coordinate is logarithmic in pressure, with an approximate vertical resolution of 1.5 km. The location of the tropopause is determined by model construction and is not interactively defined: it is forced by vertical eddy diffusion coefficients derived from the application of meteorological and dynamical data to climatological temperature fields. For this study, the model includes 60 active chemical species and 190 photochemical reactions that are treated individually rather than as chemical families. We note that there are no nonmethane hydrocarbons (NMHCs) in the model, as it is primarily a model for stratospheric chemistry and transport; thus modeled values for $\delta D_{h\nu}$ represent the isotopic composition of H_2 produced from CH_4 oxidation and include no contribution from the oxidation of NMHCs. We also note that, while 3-D models may better represent dynamical processes such as stratosphere-troposphere exchange and convective transport than do 2-D models, our previous CH_4 isotope studies [*McCarthy et al.*, 2001, 2003] have shown that model chemistry and transport are sufficient to represent the processes of interest for this study. Furthermore, the relative simplicity of a 2-D model allows us to perform numerous sensitivity studies at significantly reduced computational expense, an important practical advantage given the large uncertainties in the range of possible isotope effects that may control values for δD-H_2 and δD_{hv} in the stratosphere and troposphere.

[6] Since we compare our model predictions to observations of δD-H_2 in the stratosphere, we do not explicitly include latitude-dependent source and sink fluxes for H_2 and HD at the surface in the model. Instead, we fix the H_2 and HD mixing ratios at the surface (0–1.5 km) at values that correspond to their tropospheric global averages. This approach is sufficient for accurately representing air entering the model stratosphere, as we have shown previously for methane isotopic compositions (see *McCarthy et al.* [2003] for a comparison and discussion of model runs in which fixed surface values for CH_4 were used versus those in which latitude-dependent source and sink fluxes were used). Specifically, for all model scenarios described below, the H_2 mixing ratio was prescribed to be 0.510 ppmv (micromoles/mole) at the surface. For comparison, the globally averaged H_2 mixing ratio reported for the 1980s was 0.515 ppm [*Khalil and Rasmussen*, 1990], the average of Mace Head (53°N) and Cape Grim (41°S) measurements from 1994 to 1998 was 0.512 ppm [*Simmonds et al.*, 2000], and NOAA CMDL measurements from 1991 to 1996 were 0.530–0.535 ppm [*Novelli et al.*, 1999]. These small differences in mixing ratios at the surface have a negligible impact on modeled stratospheric H_2 mixing ratios and δD values. The HD mixing ratio was prescribed to be 180 pptv (picomoles/mole) at the surface such that δD-H_2 at the surface was equivalent to the global mean tropospheric value of 130‰ reported by *Gerst and Quay* [2000]. The δD-H_2 values reported here are from 6-year runs of LOTUS and are on average within ~1‰ of their steady state values (e.g., 50-year model integrations).

Table 2. CH_4 and H_2 Oxidation Reactions

Reaction	Deuterium-Substituted Reaction
(R1a)[a] $CH_4 + OH, Cl, O(^1D) \rightarrow CH_3 + products$	(R1b)[a] $CH_3D + OH, Cl, O(^1D) \rightarrow CH_2D + products$
	(R1c)[a] $CH_3D + OH, Cl, O(^1D) \rightarrow CH_3 + products$
(R2a)[b] $CH_4 + O(^1D) \rightarrow CH_3O + H$	(R2b)[b] $CH_3D + O(^1D) \rightarrow CH_2DO + H$
	(R2c)[b] $CH_3D + O(^1D) \rightarrow CH_3O + D$
(R3a)[b] $CH_4 + O(^1D) \rightarrow CH_2O + H_2$	(R3b)[b] $CH_3D + O(^1D) \rightarrow CHDO + H_2$
	(R3c)[b] $CH_3D + O(^1D) \rightarrow CH_2O + HD$
(R4a) $CH_3 + O_2 \rightarrow CH_3O_2$	(R4b) $CH_2D + O_2 \rightarrow CH_2DO_2$
(R5a) $CH_3O_2 + NO \rightarrow CH_3O + NO_2$	(R5b) $CH_2DO_2 + NO \rightarrow CH_2DO + NO_2$
(R6a) $CH_3O_2 + HO_2 \rightarrow CH_3OOH + O_2$	(R6b) $CH_2DO_2 + HO_2 \rightarrow CH_2DOOH + O_2$
(R7a) $CH_3OOH + OH \rightarrow CH_3O_2 + H_2O$	(R7b) $CH_2DOOH + OH \rightarrow CH_2DO_2 + H_2O$
(R8a) $CH_3OOH + h\nu \rightarrow CH_3O + OH$	(R8b) $CH_2DOOH + h\nu \rightarrow CH_2DO + OH$
(R9a) $CH_3O + O_2 \rightarrow CH_2O + HO_2$	(R9b) $CH_2DO + O_2 \rightarrow CHDO + HO_2$
	(R9c) $CH_2DO + O_2 \rightarrow CH_2O + DO_2$
(R10a)[a] $CH_2O + OH, Cl, Br, O(^3P) \rightarrow products$	(R10b)[a] $CHDO + OH, Cl, Br, O(^3P) \rightarrow products$
(R11a) $CH_2O + h\nu \rightarrow H_2 + CO$	(R11b) $CHDO + h\nu \rightarrow HD + CO$
(R12a) $CH_2O + h\nu \rightarrow H + HCO$	(R12b) $CHDO + h\nu \rightarrow H + DCO$ or $D + HCO$
(R13a)[a] $H_2 + OH, Cl, O(^1D) \rightarrow products$	(R13b)[a] $HD + OH, Cl, O(^1D) \rightarrow products$

[a]OH, Cl, $O(^1D)$, and Br reactions are also described in Table 3; products are not listed.
[b]Minor reaction channel: (R2) = 20%, (R3) = 5% of $O(^1D)$ CH_4 reaction.

[7] The photochemical reactions that control the concentration and isotopic composition of H_2 in the stratosphere are listed in Table 2. Reactions of the nondeuterated species, shown on the left side of Figure 1, are labeled with an "a" in Table 2 and are discussed first. Photochemical production of H_2 begins with abstraction of an H atom from CH_4 by OH, $O(^1D)$ or Cl (R1a) to form a methyl radical. The methyl radical produced in (R1a) is rapidly transformed into a methyl peroxy radical by reaction with O_2 (R4a). (Note that (R2a) and (R3a) in Table 2 are minor channels of the $CH_4 + O(^1D)$ reaction, accounting for 20% and 5% of the $CH_4 + O(^1D)$ products, respectively [*Sander et al.*, 2006]). The methyl peroxy radical from (R4a) can form formaldehyde (CH_2O) by a series of fast reactions ((R5a)–(R9a)). Photolysis of formaldehyde produces either H_2 + CO ((R11a), the "molecular channel") or H + HCO ((R12a), the "radical channel"). The oxidation of formaldehyde by OH, Cl, $O(^3P)$ and Br (R10a) also produces radical products but no H_2. Thus both formaldehyde oxidation and photolysis to the radical channel remove CH_2O without producing H_2. Reactions of the singly deuterated species are shown on the right side of Figure 1, are labeled "b" in Table 2, and are analogous to the reactions outlined above. Note that in several reactions oxidation of the deuterated species can, instead of abstracting a hydrogen atom, irreversibly abstract a deuterium atom. These reactions, labeled "c" in Table 2, cannot lead to production of HD (with the exception of (R3c)) and are represented by arrows crossing from the right to the left of Figure 1. They include (R1c), (R2c), (R3c), and (R9c).

[8] Importantly, accurately predicting the isotopic composition of stratospheric H_2 requires knowledge of the rate coefficients for many of the reactions in Table 2. However, many of the rate coefficients for the deuterated reactions are not known. Thus a number of model scenarios were designed to evaluate the importance of the following possible isotope effects in determining the isotopic composition of H_2 in the stratosphere and $\delta D_{h\nu}$: (1) branching ratios along the pathway from CH_3D to HD (i.e., the ratios of rate coefficients of channels b versus c for (R1), (R2), (R3), and (R9) in Table 2), (2) KIEs for formaldehyde oxidation, (3) isotope effects (IEs) in formaldehyde photolysis, and KIEs for (4) H_2 and (5) CH_4 oxidation. In sections 2.1 to 2.6, we describe current knowledge of these isotope effects and the model scenarios used to evaluate their possible influence on δD-H_2 and $\delta D_{h\nu}$. In section 2.7 we discuss the possible influence of an isotopically light source of H_2 from H_2O photolysis in the mesosphere on

Table 3. Kinetic Isotope Effects for CH_4, CH_2O, and H_2 Reactions

Reaction	KIE (k_H/k_D)	KIE at 225 K	KIE at 296 K	Reference
CH_4 + OH	0.91exp(75 ± 118/T)[a]	1.27	1.17	*DeMore* [1993]
	1.09exp(49 ± 22/T)	1.36	1.29	*Gierczak et al.* [1997]
		· · ·	1.294	*Saueressig et al.* [2001]
CH_4 + Cl	1.278exp(51.3 ± 19.1/T)[b]	1.61	1.508	*Saueressig et al.* [1996]
	0.894exp(145 ± 42/T)	1.70	1.474	*Tyler et al.* [2000]
CH_4 + $O(^1D)$	1.06[b]	1.06	1.06	*Saueressig et al.* [2001]
CH_2O + OH	1.28 ± 0.01[c]	· · ·	1.28	*Feilberg et al.* [2004]
	1	· · ·	1	*Morris and Niki* [1971]
	1.39[d]	· · ·	1.39	*D'Anna et al.* [2003]
CH_2O + Cl	1.201 ± 0.002[c]	· · ·	1.201	*Feilberg et al.* [2004]
CH_2O + Br	3.27 ± 0.03[c]	· · ·	3.27	*Feilberg et al.* [2004]
CH_2O + $O(^3P)$	2[c]	· · ·	2	*Niki et al.* [1969]
H_2 + OH	1.08exp(130 ± 25/T)[e]	1.92	1.68	*Talukdar et al.* [1996]
	1.65 ± 0.05	· · ·	1.65	*Ehhalt et al.* [1989]
H_2 + Cl	(1.75 ± 0.24)exp(80 ± 30/T)	2.5	2.3	*Taatjes* [1999]
	(1.24 ± 0.03)exp(256 ± 2/T)[e]	3.9	2.9	*Bigeleisen et al.* [1959], *Persky and Klein* [1966]
H_2 + $O(^1D)$	1 ± 0.1[e]	· · ·	1	*Talukdar and Ravishankara* [1996]

[a]Used in all model simulations except S4*, S10*, S3**, and S5**.
[b]Used in all model simulations except S3** and S5**.
[c]Used in S4, S4*, S10, and S10*.
[d]Quantum calculation.
[e]Used in all model simulations except S9.

values for stratospheric δD-H_2. In section 2.8, we discuss our method for calculating values for $\alpha_{CH4\rightarrow H2}$ and $\delta D_{h\nu}$ and evaluating their sensitivity to branching ratios from CH_3D to HD, IEs in CH_2O photolysis, and KIEs for CH_2O, H_2, and CH_4 oxidation.

2.1. Branching Ratios for H Versus D Abstraction in the Oxidation of CH_3D to HD

[9] KIEs for a number of the reactions in the chain of CH_4 oxidation reactions listed in Table 2 have been measured, for example, the ratio of rate coefficients for the reaction of CH_4 and CH_3D with OH, or $k_{CH4+OH}/k_{CH3D+OH} = k(OH)_{R1a}/(k(OH)_{R1b}+k(OH)_{R1c})$, by *DeMore* [1993] and *Gierczak et al.* [1997], as shown in Table 3. However, for several of the CH_3D oxidation reactions ((R1), (R2), (R3), and (R9)), there are two possible sets of products: one in which the deuterium is retained by the carbon fragment ((R1b), (R2b), (R3b), and (R9b)) and one in which the deuterium is abstracted and lost ((R1c), (R2c), (R3c), and (R9c)). We refer to the ratio of the rate coefficients for reaction channel b (deuterium retained by carbon fragment) to reaction channel c (deuterium abstracted and lost) for these reactions as the ''branching ratio'' for that reaction. Since no experimental values for the branching ratios exist, we must base our sensitivity studies on an unpublished value, calculated using semiclassical variational transition state theory, for the branching ratio for CH_3D + OH (i.e., $k_{R1b}(OH):k_{R1c}(OH)$) of approximately 10:1 at 250 K, thus favoring H over D atom abstraction by a factor of ~10 (J. Espinosa-Garcia, Universidad de Extremadura, Badajoz, Spain, personal communication, 2006). Note that this 10:1 branching ratio is significantly greater than the statistical branching ratio of 3:1 for (R1) that would result if each hydrogen had an equal probability of being abstracted. It is likewise expected that the branching ratios for (R1) with Cl and $O(^1D)$ as reactants, as well as for (R2), (R3), and (R9), will be greater than their statistical values since deuterium is more strongly bound than hydrogen because of a lower zero point energy.

[10] The sensitivity of modeled stratospheric δD-H_2 to choices for the magnitudes of the branching ratios along the CH_3D oxidation pathway is investigated using scenarios S1–S3. In S1, we assume that the branching ratios are statistical on the basis of the number of hydrogen sites in the molecule (see Table 4). S1 thus represents the minimum deuterium retention in the oxidation pathway leading to HD production. Conversely, in S2 we consider maximum deuterium retention in the production of HD by assuming that all the branching ratios are 1:0; that is, only hydrogen abstraction (channel b) reactions occur. In S3, we use branching ratios intermediate between S1 and S2. For the reaction CH_3D + OH we use the branching ratio of 10:1 ($k_{R1b}(OH):k_{R1c}(OH)$) calculated by Espinosa-Garcia. This branching ratio is significantly larger than the statistical 3:1 branching ratio used in S1 but smaller than the ratio of 1:0 in S2. Because no other experimental or theoretical values are available, in S3 we arbitrarily extend the 10:1 branching ratio for CH_3D + OH to CH_3D + Cl and CH_3D + $O(^1D)$ in (R1) as well as to CH_2DO + O_2 (R9); see Table 4. The branching ratios for the minor $O(^1D)$ channels in CH_4 oxidation ((R2) and (R3)) were also increased from their statistical values to arbitrary values of 3:1 and 4.6:1, respectively; the 3:1 branching ratio for (R3) was chosen to be lower than that used for (R1) by a factor of approximately 3 because of its lower statistical branching ratio (1:1 for (R3) versus 3:1 for (R1)). In the atmosphere, (R2) is rapidly followed by (R9), and the branching ratio of 4.6:1 for (R2) was chosen so that the ratio of CHDO to CH_2O produced in the reaction sequence (R2) followed by (R9) is 3:1. However, we note that setting the branching ratios for both (R2) and (R3) to 10:1 changes predicted δD-H_2 by less than 5‰, which is small compared to the differences in predicted δD-H_2 values between S1 and S2 and is also smaller than the estimated measurement precision for δD-H_2 of ±7‰ [*Rahn et al.*, 2002] and the differences in duplicate δD-H_2 measurements on the same stratospheric sample, which are as large as ~30‰ [*Rahn et al.*, 2003]. Although

Table 4. Model Scenario Parameters[a]

	Branching Ratios	CH_2O + ox KIEs[b]	CH_2O + hν IEs	H_2 Oxidation KIEs	CH_4+OH KIE
S1	**R1(b:c) 3:1, R2(b:c) 3:1, R3(b:c) 1:1, R9(b:c) 2:1**	1	1	from Table 3	*DeMore* [1993]
S2	**R1(b:c) 1:0, R2(b:c) 1:0, R3(b:c) 1:0, R9(b:c) 1:0**	1	1	from Table 3	*DeMore* [1993]
S3	**R1(b:c) 10:1, R2(b:c) 4.6:1, R3(b:c) 3:1, R9(b:c) 10:1**	1	1	from Table 3	*DeMore* [1993]
S3**	same as S3	1	1	from Table 3	**all CH_4 + ox KIEs = 1**
S4	same as S3	**OH = 1.28, Cl = 1.201, Br = 3.27, O(^{3}P) = 2**	1	from Table 3	*DeMore* [1993]
S4*	same as S3	same as S4	1	from Table 3	*Gierczak et al.* [1997]
S5	same as S3	1	**J_{R11a}/J_{R11b} = 1.25, J_{R12a}/J_{R12b} = 1.98**	from Table 3	*DeMore* [1993]
S5**	same as S3	1	same as S5	from Table 3	**all CH_4 + ox KIEs = 1**
S6	same as S3	1	**J_{R11a}/J_{R11b} = 1.40, J_{R12a}/J_{R12b} = 1.52**	from Table 3	*DeMore* [1993]
S7	same as S3	1	**$\Phi_{R11a}/\Phi_{R11b} = 1.5 \cdot \exp[-0.15\exp(E_{h\nu}-5.6)]$,[c] $\Phi_{R12a}/\Phi_{R12b} = 2.0 \cdot \exp[-0.20(E_{h\nu}-5.6)]$[c]**	from Table 3	*DeMore* [1993]
S7a	same as S3	1	**J_{R11a}/J_{R11b} = 1.41, J_{R12a}/J_{R12b} = 1.71**	from Table 3	*DeMore* [1993]
S8	same as S3	1	**σ(CHDO), Φ_{R11b}, and Φ_{R12b} blue-shifted by ~1.43 kcal/mol with respect to $\sigma(CH_2O)$, Φ_{R11a}, and ΦR_{12a}**	from Table 3	*DeMore* [1993]
S8a	same as S3	1	**J_{R11a}/J_{R11b} = 1.11, J_{R12a}/J_{R12b} = 1.41**	from Table 3	*DeMore* [1993]
S9	same as S3	1	1	**1**	*DeMore* [1993]
S10	same as S3	same as S4	same as S5	from Table 3	*DeMore* [1993]
S10*	same as S3	same as S4	same as S5	from Table 3	*Gierczak et al.* [1997]

[a]Boldface highlights the particular isotope effect(s) that was changed/tested for each model scenario.
[b]ox = OH, Cl, Br, or O(1D).
[c]$E_{h\nu}$ is the photon energy in units of 10^{-19} J/molecule.

a number of the values for the branching ratios in S3 are arbitrary, these values are carried through in S4–S10 (see Table 4), in part because the maximum and minimum deuterium retention branching ratios in S1 and S2 appear to be unrealistic both with respect to theoretical predictions for CH_3D + OH and with respect to predicting δD-H_2 values consistent with the ER-2 observations, as we will show in section 3.

2.2. KIEs for Formaldehyde Oxidation

[11] All the KIEs for the oxidation reactions that destroy formaldehyde (i.e., k_{R10a}/k_{R10b} for the reactions with OH, O(^{3}P), Cl, and Br) preferentially destroy the light CH_2O isotopomer, enriching the remaining formaldehyde in deuterium and thereby resulting in larger values for $\delta D_{h\nu}$ and δD-H_2 than in the absence of any KIEs for CH_2O oxidation. Recently measured values for the hydrogen KIEs for CH_2O oxidation by OH, Cl and Br are 1.28 ± 0.01, 1.201 ± 0.002 and 3.27 ± 0.03, respectively, on the basis of relative rate experiments at room temperature using long-path FTIR detection [*Feilberg et al.*, 2004]. While these are the only experimental KIEs available for CH_2O + Cl and CH_2O + Br, the CH_2O + OH KIE was also the subject of a 1971 experiment which found no difference in the rate coefficients for CH_2O versus CHDO [*Morris and Niki*, 1971]. However, Morris and Niki estimated 25% uncertainties in the individual rate coefficients and the data points for the CHDO reaction were quite limited in number, both suggesting that a KIE for the reaction was simply not measurable in their experiment. Moreover, a recent quantum calculation for the CH_2O + OH KIE yielded a value of 1.39 [*D'Anna et al.*, 2003], a result within 8% of the value of 1.28 determined experimentally by *Feilberg et al.* [2004]. For reaction of CH_2O with O(^{3}P), a KIE of 2 was reported in a conference proceeding [*Niki et al.*, 1969], although this value remains uncorroborated. A summary of these KIEs is given in Table 3. In our model, we evaluate the sensitivity of δD-H_2 to KIEs in formaldehyde oxidation by comparing scenarios S3 and S4. In S3 (as in S1 and S2), these KIEs are all set to 1. In S4, we use the *Feilberg et al.* [2004] KIEs for reaction of CH_2O with OH, Cl and Br, the O(^{3}P) KIE from *Niki et al.* [1969], and the S3 branching ratios discussed in the previous section.

2.3. Isotope Effects in Formaldehyde Photolysis

[12] Photolysis of formaldehyde, which occurs at wavelengths between about 240 and 360 nm, is the primary pathway by which CH_4 oxidation produces H_2 (with only a small contribution from (R3)). For this reason, any isotope effects in formaldehyde photolysis ((R11) and (R12)) have the potential to significantly affect values for $\delta D_{h\nu}$ and δD-H_2. Photolysis of formaldehyde can either yield molecular (R11) or radical (R12) products; the radical channel has a higher dissociation threshold and is thus favored at short wavelengths while the molecular channel is favored at the longer wavelengths that predominate in the troposphere and stratosphere. As a result of this wavelength dependence, both the absolute and relative magnitudes of the molecular versus radical channel J-values vary with latitude and altitude. Isotope effects in formaldehyde photolysis (that is, ratios of J-values for CH_2O versus CHDO) are not well characterized and could result from differences in the absorption cross sections for CH_2O and CHDO and/or from differences in the CH_2O versus CHDO quantum yields for the molecular and radical channels. Thus accurately simulating the ratio of HD to H_2 produced from CH_2O photolysis requires either knowledge of all of these quantities as a function of wavelength and possibly their dependence on temperature and pressure and/or evidence that any differences in such properties between the isotopomers do not result in significant differences in $\delta D_{h\nu}$ and δD-H_2 in different regions of the atmosphere.

[13] While absorption cross sections and quantum yields have been measured for CH_2O [see, e.g., *Moortgat et al.*, 1983], these quantities have not been explicitly published for CHDO. Thus, since we currently have no direct knowledge of IEs in formaldehyde photolysis, we must instead create model scenarios to test the sensitivity of $\delta D_{h\nu}$ and δD-H_2 to possible photolysis IEs by drawing on insight from several relevant experiments and theoretical calculations. While none of the studies we highlight below provide the direct information needed to model $\delta D_{h\nu}$ and δD-H_2 on a molecular level, they all suggest that CH_2O is more rapidly photolyzed than CHDO and that CH_2O photolysis leads to H_2 that is isotopically lighter than the formaldehyde from which it is produced, at least for conditions at Earth's surface. As discussed below, we choose parameters for the model scenarios that are as consistent as possible with the constraints provided by theory and experiment available to date.

[14] Several experiments performed in sunlight at the surface provide constraints on the magnitudes of the IEs for formaldehyde photolysis. The ratio of first-order rate coefficients for CH_2O versus CHDO photolysis, $(J_{R11a} + J_{R12a})/(J_{R11b} + J_{R12b})$, was recently estimated to be 1.44 in such an experiment (C. J. Nielsen, personal communication, 2006). This experimentally derived ratio indicates that CH_2O is photolyzed more rapidly than CHDO but does not provide any information about the distribution of radical and molecular products. Note that in order to model the HD/H_2 ratio produced by CH_2O photolysis, however, the values of the IEs for both the molecular and radical channels, i.e., J_{R11a}/J_{R11b} and J_{R12a}/J_{R12b}, respectively, are needed. Unfortunately, these are not uniquely determined by the value for $(J_{R11a} + J_{R12a})/(J_{R11b} + J_{R12b})$ measured by Nielsen and coworkers, and there are ranges of molecular and radical channel IEs that are consistent with this measured ratio. In another experiment in which formaldehyde was photolyzed in sunlight at the surface, *Crounse et al.* [2003] measured the D/H ratio of H_2 produced and found that it was 200‰ lighter than that of the initial formaldehyde; from this they estimated that the value of J_{R11a}/J_{R11b} is 1.25. This result is consistent with the more rapid photolysis of CH_2O than CHDO observed by Nielsen. We use the constraints on $(J_{R11a} + J_{R12a})/(J_{R11b} + J_{R12b})$ and J_{R11a}/J_{R11b} provided by the Nielsen and Crounse et al. experiments in S5, discussed in more detail at the end of this section. However, because the isotope effects for CH_2O photolysis may be wavelength-dependent, there is uncertainty associated with applying measurements from surface experiments to the stratosphere, as discussed below.

[15] In addition to the constraints on the ratios of J values for CH_2O photolysis provided by the experiments of Nielsen and coworkers and *Crounse et al.* [2003], the experiments of *McQuigg and Calvert* [1969] provide some information on the molecular and radical channel quantum yields for CH_2O and CHDO. Note that the relationship between J-values, absorption cross sections, and quantum yields is described by equation (1), where σ is the absorption cross section, Φ is the quantum yield, I is the spectral actinic flux, and λ and T refer to wavelength and temperature, respectively.

$$J = \int_{\lambda_1}^{\lambda_2} \sigma(\lambda, T) \cdot \phi(\lambda, T) \cdot I(\lambda) d\lambda \quad (1)$$

McQuigg and Calvert [1969] measured the volumes of H_2, HD, D_2, and CO following photolysis of CH_2O or CHDO with a xenon flashlamp. They reported that the total CHDO photolysis quantum yield (the sum of both molecular and radical channels) is lower than that for CH_2O (i.e., $\Phi_{R11b} + \Phi_{R12b} < \Phi_{R11a} + \Phi_{R12a}$), on the basis of a model of the chemistry occurring in their reaction cell. While these values have large uncertainties due to approximations made in their photochemical model and impurities in their CHDO sample, this result is also consistent with more rapid photolysis of CH_2O than CHDO (but note that calculation of the ratios of J-values from the quantum yields requires knowledge of the relative absorption cross sections for CH_2O versus CHDO; see equation (1)). They also reported that the ratio of molecular to radical channel quantum yields, integrated over wavelengths between 260 and 360 nm, is higher for deuterated than for nondeuterated formaldehyde ($\Phi_{R11b}/\Phi_{R12b} = 1.7 > \Phi_{R11a}/\Phi_{R12a} = 1.4$), although it is unclear if these numbers are significantly different within their error. This latter result is algebraically equivalent to having Φ_{R12a}/Φ_{R12b} (the ratio of CH_2O versus CHDO quantum yields for the radical channel) be greater than Φ_{R11a}/Φ_{R11b} (the ratio of quantum yields for the molecular channel). Because of the large uncertainties, we do not use the wavelength-integrated values for Φ_{R11b}/Φ_{R12b} and Φ_{R11a}/Φ_{R12a} determined by McQuigg and Calvert directly in our model simulations, but we do examine the effect of changing the relative magnitudes of the radical versus molecular channel IEs using scenarios S5 and S6, discussed below. We expect the role of a radical channel IE

Table 5. Summary of Parameters for CH_2O Photolysis Scenarios

	CH_2O Photolysis IE	Range for Ratios of Φs	Range for Ratios of J Values	Average Ratios of J Values[a]	Other Constraints
S5	$J_{R11a}/J_{R11b} = 1.25$, $J_{R12a}/J_{R12b} = 1.98$				$\frac{(J_{R11a}+J_{R12a})}{(J_{R11b}+J_{R12b})} = 1.44$
S6	$J_{R11a}/J_{R11b} = 1.40$, $J_{R12a}/J_{R12b} = 1.52$				$\frac{(J_{R11a}+J_{R12a})}{(J_{R11b}+J_{R12b})} = 1.44$
S7	$\Phi_{R11a}/\Phi_{R11b} = 1.5\cdot\exp[-0.15(E_{h\nu} - 5.6)]$,[b] $\Phi_{R12a}/\Phi_{R12b} = 2.0\cdot\exp[-0.20(E_{h\nu} - 5.6)]$[b]	Φ_{R11a}/Φ_{R11b}: 1.5 to 1.0 (355 to 242 nm), Φ_{R12a}/Φ_{R12b}: 1.9 to 1.2 (345 to 242 nm)	J_{R11a}/J_{R11b}: 1.37 to 1.45, J_{R12a}/J_{R12b}: 1.66 to 1.82	$(J_{R11a}/J_{R11b})_{avg} = 1.41$, $(J_{R12a}/J_{R12b})_{avg} = 1.71$	
S7a	$J_{R11a}/J_{R11b} = 1.41$, $J_{R12a}/J_{R12b} = 1.71$				same as the average IEs for S7
S8	σ(CHDO), Φ_{R11b}, and Φ_{R12b} blue-shifted by ~1.43 kcal/mol with respect to $\sigma(CH_2O)$, Φ_{R11a}, and ΦR_{12a}		J_{R11a}/J_{R11b}: 1.08 to 1.29, J_{R12a}/J_{R12b}: 1.17 to 2.81	$(J_{R11a}/J_{R11b})_{avg} = 1.11$, $(J_{R12a}/J_{R12b})_{avg} = 1.41$	
S8a	$J_{R11a}/J_{R11b} = 1.11$, $J_{R12a}/J_{R12b} = 1.41$				same as the average IEs for S8

[a] $(J_{R11a}/J_{R11b})_{avg}$ and $(J_{R12a}/J_{R12b})_{avg}$ are the globally averaged ratios of J values (where the average is taken over latitude, altitude and season) calculated by the model for scenarios where Φ_{R11a}/Φ_{R11b} and Φ_{R12a}/Φ_{R12b} are wavelength-dependent.
[b] $E_{h\nu}$ is the excitation energy in units of 10^{-19} J/molecule.

to be analogous to the effect of the KIEs for CH_2O oxidation discussed in section 2.2: a radical channel IE that is greater than 1 enriches formaldehyde in deuterium without forming H_2 or HD, thus making the H_2 produced by the competing molecular channel heavier.

[16] While there may be isotopic differences in the absorption cross sections and quantum yields which are wavelength-dependent and which may therefore play out differently in different regions of the atmosphere, we have found no direct experimental evidence for or against a wavelength dependence for the isotope effects for CH_2O photolysis. *Rhee et al.* [2006b] have suggested that the experimental results of *McQuigg and Calvert* [1969] demonstrate there is no wavelength dependence, but the corresponding uncertainties are large and we believe no conclusion can be drawn either way. However, some insight is provided by the work of *Miller* [1979], who calculated isotope effects in the decomposition of energetically excited CH_2O and CD_2O to molecular products using tunneling corrections to RRKM theory. He found that the magnitude of $k_{CH2O}(E)/k_{CD2O}(E)$, i.e., the ratio of microcanonical rate coefficients, varies by a factor of more than 5 over the range of total energies from 90 to 120 kcal/mol relative to the minimum of the formaldehyde potential energy surface (meaning that the ZPEs of the different isotopomers are not included), corresponding to wavelengths of 387–275 nm for CH_2O and 371–267 nm for CD_2O. Specifically, $k_{CH2O}(E)/k_{CD2O}(E)$ is ~4 at a total energy of 90 kcal/mol and decreases exponentially with total energy to ~0.7 at ~100 kcal/mol, while above 105 kcal/mol the ratio is a fairly flat function of energy and close to a value of 1 [see *Miller*, 1979]. A transformation of Miller's calculated ratios of k(E)s to ratios of molecular channel quantum yields as a function of wavelength and temperature (i.e., $\Phi(\lambda, T)$), however, is not straightforward. In addition, Miller's calculations provide no information regarding the absorption cross sections of CH_2O, CHDO, or CD_2O. For these reasons, we cannot use his results directly in our model, although we can examine the sensitivity of modeled δD-H_2 and $\delta D_{h\nu}$ to hypothetical CH_2O photolysis isotope effects that change as a function of photon energy based qualitatively on Miller's calculations, as discussed below.

[17] In order to test the effect of possible IEs for formaldehyde photolysis on δD-H_2 and $\delta D_{h\nu}$, we created scenarios S5–S8 on the basis of the constraints on the IEs for CH_2O photolysis provided by the experiments and theory discussed above. In all scenarios, CH_2O photolysis is faster than CHDO photolysis (i.e., $J_{R11a}/J_{R11b} > 1$ and $J_{R12a}/J_{R12b} > 1$). In S5, we use the two currently unpublished values discussed above for J_{R11a}/J_{R11b} and $(J_{R11a} + J_{R12a})/(J_{R11b} + J_{R12b})$ as a logical starting point: the value for J_{R11a}/J_{R11b} (the molecular channel IE) of 1.25 estimated by *Crounse et al.* [2003] and the constraint on the ratio of photolysis rate coefficients measured by Nielsen and coworkers of $(J_{R11a} + J_{R12a})/(J_{R11b} + J_{R12b}) = 1.44$. In order to derive a value for the radical channel IE (J_{R12a}/J_{R12b}) on the basis of these two constraints from surface experiments, we also use the fact that the average value of J_{R11a}/J_{R12a}, the ratio of molecular to radical products produced by CH_2O, was 1.80 in the experiment of Nielsen and coworkers (C. J. Nielsen, personal communication, 2006), which is close to a value of 1.76 calculated by our model for the surface at 32.5°N in April on the basis of measured absorption cross sections and quantum yields for CH_2O as a function of wavelength, temperature, and pressure. (We note that in the experiments of Nielsen and coworkers, J_{R11a}/J_{R12a} varied from 1.65 to 1.95 over the course of the experiment but that this range of values changes predicted δD-H_2 by less than 5‰.) In the model, J_{R11a}/J_{R12a} increases with altitude to a maximum of 2.39 at 20.25 km at 32.5°N and then decreases to 1.31 at 39.75 km; the range from tropics to poles is ~1.6 to ~3 at the surface, respectively, with a similar range in seasonality. Using these 3 constraints derived from surface observations, $J_{R11a}/J_{R11b} = 1.25$, $(J_{R11a} + J_{R12a})/(J_{R11b} + J_{R12b}) = 1.44$, and $J_{R11a}/J_{R12a} = 1.80$, we calculate that the value for J_{R12a}/J_{R12b} is 1.98 and use this value in S5 (see Tables 3 and 5). In S6, we test the effect of decreasing the radical channel IE (J_{R12a}/J_{R12b}), still using the constraints $(J_{R11a} + J_{R12a})/(J_{R11b} + J_{R12b}) = 1.44$ and $J_{R11a}/J_{R12a} = 1.80$. As a sensitivity test, we arbitrarily choose $J_{R11a}/J_{R11b} = 1.40$ (a value that is larger than 1.25 and that also keeps the

magnitude of the resulting isotope effects between 1 and 2), which gives J_{R12a}/J_{R12b} a value of 1.52 (see Tables 3 and 5). Note that for both S5 and S6, the radical channel IE (J_{R12a}/J_{R12b}) is larger than the molecular channel IE (J_{R11a}/J_{R11b}), consistent with the *McQuigg and Calvert* [1969] result. Finally, we note that in S5 and S6 we are assuming that the value for $(J_{R11a} + J_{R12a})/(J_{R11b} + J_{R12b})$ measured by Nielsen and coworkers at the surface is the same throughout the troposphere and stratosphere and that the ratios of J-values (i.e., the isotope effects) for the molecular and radical channels for CHDO versus CH_2O in S5 and S6 are also constant (although the individual J-values for CH_2O and CHDO photolysis both vary with latitude and altitude).

[18] In contrast to assuming that ratios of J-values for the CHDO versus CH_2O isotopologues are constant throughout the atmosphere, in S7 and S8 we allow the IEs for CH_2O photolysis to be wavelength-dependent. In S7, the ratios of the CH_2O versus CHDO quantum yields for the molecular and radical channels (i.e., Φ_{R11a}/Φ_{R11b} and Φ_{R12a}/Φ_{R12b}) decrease exponentially with photon energy, which is the trend calculated for $k_{CH2O}(E)/k_{CD2O}(E)$ for total energies below 100 kcal/mol by *Miller* [1979]. The ratios of quantum yields for the molecular and radical channels used in S7 are described by equations (2) and (3), respectively.

$$\frac{\Phi_{R11a}}{\Phi_{R11b}} = 1.5 \times \exp[-0.15 \times (E_{h\nu} - 5.6)] \quad (2)$$

$$\frac{\Phi_{R12a}}{\Phi_{R12b}} = 2.0 \times \exp[-0.20 \times (E_{h\nu} - 5.6)] \quad (3)$$

Here, $E_{h\nu}$ is the photon energy and 5.6 corresponds to the energy of a 355 nm photon, both in units of 10^{-19} Joules/molecule. The form and values in equations (2) and (3) were chosen so that the magnitudes of Φ_{R11a}/Φ_{R11b} and Φ_{R12a}/Φ_{R12b} arbitrarily range between 1 and 2 from 242 to 355 nm and so that the ratio Φ_{R11a}/Φ_{R11b}:Φ_{R12a}/Φ_{R12b} varies as a function of wavelength. As in S5 and S6, in S7 we have chosen the magnitude of Φ_{R11a}/Φ_{R11b} (molecular channel) to be smaller than that for Φ_{R12a}/Φ_{R12b} (radical channel), consistent with *McQuigg and Calvert* [1969]. Note that a wavelength-dependent isotope effect for formaldehyde photolysis will depend on how the product of the ratio of the isotope-specific quantum yields (Φ_{R11a}/Φ_{R11b} or Φ_{R12a}/Φ_{R12b}) and the ratio of the isotope-specific absorption cross sections ($\sigma_{CH2O}/\sigma_{CHDO}$) varies as a function of wavelength and not just on the ratio of the isotope-specific quantum yields (Φ_{R11a}/Φ_{R11b} or Φ_{R12a}/Φ_{R12b}). However, since the CHDO absorption cross sections are not available, we assume for this scenario that they are equivalent to the CH_2O cross sections. Specifically, for the molecular channel in S7, the value of Φ_{R11a}/Φ_{R11b} ranges from 1.5 at 355 nm to 1.0 at 242 nm. For the radical channel, the value of Φ_{R12a}/Φ_{R12b} ranges from 1.9 at 345 nm to 1.2 at 242 nm (see Table 5). Interestingly, because of the broad range of wavelengths generally available in a model grid cell, values for J_{R11a}/J_{R11b} and J_{R12a}/J_{R12b} calculated by the model for S7 vary considerably less than do the values for Φ_{R11a}/Φ_{R11b} and Φ_{R12a}/Φ_{R12b}; they range from 1.37 to 1.45 for the molecular channel and from 1.66 to 1.82 for the radical channel (see Table 5).

[19] Values for δD-H_2 and $\delta D_{h\nu}$ predicted by S7 potentially depend on both the magnitudes of the molecular and radical channel IEs and the variation in these IEs as a function of wavelength. In order to distinguish between these two possible effects, from the model output for S7 we calculated the globally averaged values for J_{R11a}/J_{R11b} and J_{R12a}/J_{R12b}, equal to 1.41 and 1.71, respectively, with the average taken over latitude, altitude, and season, and use these averages as wavelength-independent IEs in S7a.

[20] Next, instead of explicitly varying the ratios of CH_2O versus CHDO photolysis quantum yields as in S7, we use S8 to test the effect of a photolysis IE in which the CHDO absorption cross sections and quantum yields are simply blue-shifted with respect to those for CH_2O. Since the ultraviolet absorption spectrum of CH_2O is highly structured, a possible blue shift in the spectral lines for CHDO could result in significant isotopic fractionation, although the overall effect will also depend on the actinic flux in different regions of the atmosphere and, in this study, the spectral resolution of the model. In S8, we blue-shift the CHDO absorption cross sections and molecular and radical channel quantum yields with respect to those for CH_2O by an energy of ~1.43 kcal/mol; this value was chosen as an arbitrary, small ΔE corresponding to the energy difference between centers of adjacent wavelengths bins for the majority of wavelength bins in LOTUS and equivalent to about half of the zero point energy difference between CH_2O and CD_2O [*Miller*, 1979]. This simple, zeroth-order treatment is similar to that used with qualitative success by *Yung and Miller* [1997] to describe isotope effects for the photolysis of N_2O. While this method has been shown to be overly simplified for describing isotopic shifts for N_2O and other molecules [see, e.g., *Liang et al.*, 2004; *Nanbu and Johnson*, 2004; *Prakash et al.*, 2005], S8 allows us to test the sensitivity of δD-H_2 and $\delta D_{h\nu}$ to a generalized blue-shifted photolysis isotope effect. We note that values for J_{R11a}/J_{R11b} and J_{R12a}/J_{R12b} in S8 range from 1.08 to 1.29 and 1.17 to 2.81, respectively, which are significantly larger than the ranges of ratios of J-values in S7, especially for the radical channel (Table 5). As for S7 and S7a above, to test whether the spatial and temporal variation in δD-H_2 and $\delta D_{h\nu}$ predicted by S8 are due to a wavelength dependence or simply the relative magnitudes of the IEs, we also created S8a in which wavelength-independent values of J_{R11a}/J_{R11b} and J_{R12a}/J_{R12b} are calculated from the globally averaged values from S8 (1.11 and 1.41, respectively; see Table 5).

[21] Finally, we note that it is possible that the IEs in CH_2O photolysis may be pressure- and/or temperature-dependent since the quantum yields for the CH_2O molecular channel depend on pressure and temperature for wavelengths longer than ~330 nm [*Moortgat et al.*, 1983] and the absorption cross sections of CH_2O are also temperature-dependent [*Cantrell et al.*, 1990]. However, because there is no experimental or theoretical guidance as to what the potential isotope effects may be when considering CH_2O versus CHDO, examining the effect of possible pressure- or temperature-dependent IEs is beyond the scope of this study.

2.4. KIEs for H_2 Oxidation

[22] Large KIEs in the H_2 + OH and H_2 + Cl reactions enrich stratospheric H_2 in deuterium by preferentially remov-

ing H_2 over HD. The KIE for H_2 + OH has been investigated in two laboratories [*Ehhalt et al.*, 1989; *Talukdar et al.*, 1996] (see Table 3), which agree on the value of the KIE at room temperature. For model scenarios, we use the temperature-dependent rate coefficient expression of *Talukdar et al.* [1996] based on experiments conducted between 238 and 400 K. The uncertainty in their KIE is about ±7% at 298 K and increases to ±10% at 238 K. The KIE for H_2 + Cl has been the subject of three published experiments. *Bigeleisen et al.* [1959] and *Persky and Klein* [1966] report the same temperature-dependent rate coefficient expression for the H_2 + Cl KIE, which we use in our model scenarios, based on experiments between 243 and 350 K. *Taatjes* [1999] reports another temperature-dependent expression for the KIE derived from experiments conducted between 293 and 705 K, which is smaller than the KIE determined by Bigeleisen et al. and Persky and Klein by a factor of ~1.5 at 225 K. However, we note that using the Taatjes KIE results in only a small change (<5‰ in general and <1‰ for CH_4 > 1.2 ppmv) in predicted δD-H_2. The reaction of H_2 with $O(^1D)$ has no measurable KIE, reported as 1 ± 0.1 [*Talukdar and Ravishankara*, 1996]; we use this KIE for our model scenarios. To test the importance of the KIEs for H_2 + OH and H_2 + Cl for modeled δD-H_2, both of these KIEs are set to 1 in S9.

2.5. KIEs for CH_4 + OH, Cl, and $O(^1D)$

[23] KIEs for abstracting a hydrogen atom from CH_4 by reaction with OH, Cl and $O(^1D)$ lead to preferential oxidation of nondeuterated CH_4. For a given CH_4 isotopic composition, the H_2 produced from CH_4 oxidation is considerably lighter than it would be in the absence of any of these hydrogen abstraction KIEs. However, we note that these KIEs also enrich the stratospheric methane reservoir in deuterium as the air mass ages, which tends to make the H_2 produced from CH_4 oxidation isotopically heavier for older air so that both effects are an important determinant of δD-H_2 and $\delta D_{h\nu}$ in the stratosphere, as we will show. For reaction of CH_4 with OH and Cl, different laboratories have reported significantly different hydrogen KIEs (see Table 3). As shown by *McCarthy et al.* [2003], the KIE for CH_4 + OH from *DeMore* [1993] produced better agreement between the ER-2 δD-CH_4 measurements of *Rice et al.* [2003] and the 2-D model results than the KIE from *Gierczak et al.* [1997]. However, given recent stratospheric δD-CH_4 measurements by *Rhee et al.* [2006b] that appear to be heavier by about 15–20‰ than those reported by *Rice et al.* [2003], the agreement at room temperature between the CH_4 + OH KIEs from *Gierczak et al.* [1997] and *Saueressig et al.* [2001], and potential errors in model chemistry and transport [*McCarthy et al.*, 2003], it is still unclear which KIE should be used. For simulating stratospheric δD-H_2, the differences in magnitudes and temperature dependencies of the DeMore versus the Gierczak et al. CH_4 + OH KIEs matter little, resulting in small differences in δD-H_2 of 10‰ or less. However, modeled values for $\delta D_{h\nu}$, particularly in the troposphere, are quite different, as we will show. Since the DeMore KIE produced better agreement between model results and ER-2 observations of δD-CH_4, it is used in the majority of scenarios, while two sensitivity runs were performed using the Gierczak et al. KIE; the latter are designated with an asterisk (specifically, S4* and S10*); see Tables 3 and 4. For the reaction of CH_4 with Cl, additional sensitivity runs showed that differences in measured KIEs also result in only very small differences in stratospheric δD-H_2, on the order of 10‰ each, and do not result in significantly different values for $\delta D_{h\nu}$ in the troposphere. For CH_4 + $O(^1D)$, the KIE used in all scenarios is from *Saueressig et al.* [2001], based on modeling results shown by *McCarthy et al.* [2003]. Finally, several scenarios, denoted with double asterisks (**), were run in which all the CH_4 + oxidant KIEs were set to 1.

2.6. Composite Scenario S10 and Estimating Percent Contributions to Deuterium Enrichment

[24] In addition to the model scenarios described above, we also ran S10, which includes all measured KIEs (for CH_4, CH_2O and H_2 oxidation) as noted above, the S3 branching ratios (based in part on Espinosa-Garcia's theoretical calculation for CH_3D + OH), and the constraints on the IEs for CH_2O photolysis determined experimentally by Nielsen and coworkers and *Crounse et al.* [2003] at the surface (as in S5), assuming that these surface constraints on relative J-values are valid for the stratosphere. Using results from S10 and comparisons with results from scenarios with and without the various categories of isotope effects (including additional model scenarios not shown in Table 4), we also estimated the percent contribution of each category of isotope effect to deuterium enrichment in stratospheric H_2 at a CH_4 mixing ratio of 0.8 ppmv. For example, to estimate the contribution of the CH_4 oxidation KIEs to deuterium enrichment, we compared S10 to a run in which the CH_4 oxidation KIEs are set to 1. The percent contribution was then calculated as the difference in δD-H_2 between S10 and S10 without the CH_4 oxidation KIEs divided by the difference between δD-H_2 in S10 and the average tropospheric value of 130‰. The uncertainty in the percent contribution was estimated by evaluating the effect of including versus not including the CH_4 oxidation KIEs on δD-H_2 in other scenarios (e.g., comparing S3 and S3**) and taking into account measurement uncertainties in the KIEs (e.g., measurement differences in the CH_4 + OH KIE as evaluated in S10 and S10*). The percent contributions of the other relatively well-constrained KIEs in H_2 and CH_2O oxidation and their uncertainties were estimated analogously. The uncertainties in the contribution of the CH_2O photolysis isotope effects and CH_3D oxidation branching ratios to deuterium enrichment in H_2, however, are large and interrelated: because both are underconstrained experimentally, as we will demonstrate below, both can be varied within a certain range (although not independently) and still result in δD-H_2 values that are consistent with observations. Thus our estimate of the upper bound for the contribution of the CH_3D branching ratios corresponds to the lower bound for the CH_2O photolysis isotope effects and vice versa. For the CH_2O photolysis isotope effects, our "best" estimate of their percent contribution was made using the isotope effects in S5 since they are based on the body, albeit limited, of experimental and theoretical knowledge to date. Our lower (most negative) bound on the contribution of CH_2O photolysis IEs was roughly based on the constraint of the maximum possible CH_3D oxidation branching ratios shown in S2 since, if the contribution of the CH_2O photolysis IEs to deuterium enrichment were more negative than the range

Table 6. Reactions Modified for Modeling $\delta D_{h\nu}$

Reaction	Deuterium-Substituted Reaction
(R3a′) $CH_4 + O(^1D) \rightarrow CH_2O + H_2 + HA$	(R3b′) $CH_3D + O(^1D) \rightarrow CHDO + H_2 + HA$
	(R3c′) $CH_3D + O(^1D) \rightarrow CH_2O + HD + HB$
(R11a′) $CH_2O + h\nu \rightarrow CO + H_2 + HA$	(R11b′) $CHDO + h\nu \rightarrow CO + HD + HB$

we present, then inclusion of even the maximum possible branching ratios would result in δD-H_2 that was lighter than the observations. Our upper bound to the contribution of CH_2O photolysis IEs is a rough estimate made by placing some confidence in the branching ratio for CH_3D + OH calculated by J. Espinosa-Garcia since we consider the statistical branching ratios to be an unrealistic lower bound. Finally, for each scenario we calculated the contribution of the CH_3D + OH branching ratios by difference, so that the percent contributions of each category of isotope effect sum to 100%.

2.7. H_2 Production From H_2O Photolysis in the Mesosphere and the Total Deuterium Budget

[25] Photolysis of water vapor to H + OH becomes important in the mesosphere where light with wavelengths shorter than 200 nm is readily available. The atomic hydrogen produced by H_2O photolysis can react with HO_2 to produce H_2 and O_2, making water photolysis a source of H_2 in the mesosphere. Furthermore, H_2 produced in this way is expected to be extremely isotopically light because the source H_2O in the mesosphere is light (i.e., −30 to −580‰ [see *Sandor and Clancy*, 2003]). Evidence that the effect of this source of light H_2 in the mesosphere can be measured in the stratosphere is presented in the abstract of *Rhee et al.* [2004], who report balloon-based observations of stratospheric δD-H_2 in which isotopically light H_2, deviating from the δD-H_2:CH_4 relationship that describes the rest of their data, was observed for one flight and attributed to a mesospheric intrusion. To evaluate the possible influence of a source of isotopically light H_2 in the mesosphere on the isotopic composition of H_2 in the stratosphere, we performed two simulations: one in which the isotopic composition of H_2 was fixed at −800‰ between 83.5 and 85 km in the mesosphere (the top model layer), and another in which the isotopic composition of H_2 was fixed at −200‰ between 75 and 85 km in the mesosphere. The values −200 and −800‰ were chosen as representative of a light and an extremely light source, respectively. The results of these sensitivity runs, discussed in section 3 below, show that the influence of the mesospheric source of H_2 from H_2O photolysis on the isotopic composition of H_2 for "background" stratospheric air in our model is small to negligible. Hence the fact that we do not keep track of the deuterium isotopic composition of water, both for computational efficiency and due to significant uncertainties in the processes that control the isotopic composition of water vapor entering the stratosphere [see, e.g., *McCarthy et al.*, 2004, and references therein], and thus do not conserve the total deuterium budget in the stratosphere, has a negligible effect on our model results for stratospheric δD-H_2.

2.8. Calculating $\alpha'_{CH4\rightarrow H2}$ and $\delta D_{h\nu}$

[26] For each of the model scenarios introduced above, we also calculate values for $\alpha'_{CH4\rightarrow H2}$ (the isotopic fractionation factor for the conversion of CH_4 to H_2) and $\delta D_{h\nu}$ (the isotopic composition of H_2 produced from CH_4 oxidation). Note that $\alpha'_{CH4\rightarrow H2}$ is the inverse of $\alpha_{CH4\rightarrow H2}$ defined by *Rahn et al.* [2003] and *Rhee et al.* [2006b], conforming to the standard chemists' definition of isotope effects as the H/D ratios of rate coefficients that we have used throughout this paper, rather than the standard isotope geochemists' definition as the D/H ratios. For these calculations, we add two fictitious species to the model, "HA" and "HB," which are produced as H_2 and HD are from CH_4 oxidation, respectively, but which are nonreactive and nontransported. This approach allows us to calculate values for $\alpha'_{CH4\rightarrow H2}$ and $\delta D_{h\nu}$ for a given time step in a given grid cell and to do so without affecting the concentrations of any other species. The reactions modified for these calculations are listed in Table 6 and are denoted with a prime (e.g., (R3′)). Values for $\alpha'_{CH4\rightarrow H2}$ and $\delta D_{h\nu}$ are then calculated by equations (4) and (5), respectively,

$$\alpha'_{CH4\rightarrow H2} = \frac{\left(\frac{CH_3D}{3CH_3D + 4CH_4}\right)}{\left(\frac{HB}{2HA + HB}\right)} \tag{4}$$

$$\begin{aligned}\delta D_{h\nu} &= \left[\frac{\left(\frac{HB}{2HA+HB}\right)}{\left(\frac{D}{H}\right)_{std}} - 1\right] \times 1000 \\ &= \left[\frac{1}{\alpha'_{CH4\rightarrow H2}} \times \left(1 + \frac{\delta D_{CH4}}{1000}\right) - 1\right] \times 1000\end{aligned} \tag{5}$$

where the quantities HB/(2HA + HB) and $CH_3D/(3CH_3D + 4CH_4)$ represent the elemental D/H ratios for the molecular species HA and CH_4, and $(D/H)_{std}$ is the (D/H) ratio for VSMOW of 155.76×10^{-6}. Equation (4) is the standard definition of an isotopic fractionation factor (using the light/heavy convention so that, when $\alpha'_{CH4\rightarrow H2} < 1$, the conversion of CH_4 to H_2 results in deuterium enrichment in the product H_2); thus $\alpha'_{CH4\rightarrow H2}$ reflects the change in isotopic composition ongoing from CH_4 to H_2. In contrast, equation (5) gives our definition of $\delta D_{h\nu}$ (which is simply the isotopic composition of H_2 produced from CH_4 oxidation) and shows that values for $\delta D_{h\nu}$ depend not only on the magnitude of the underlying fractionation factor,

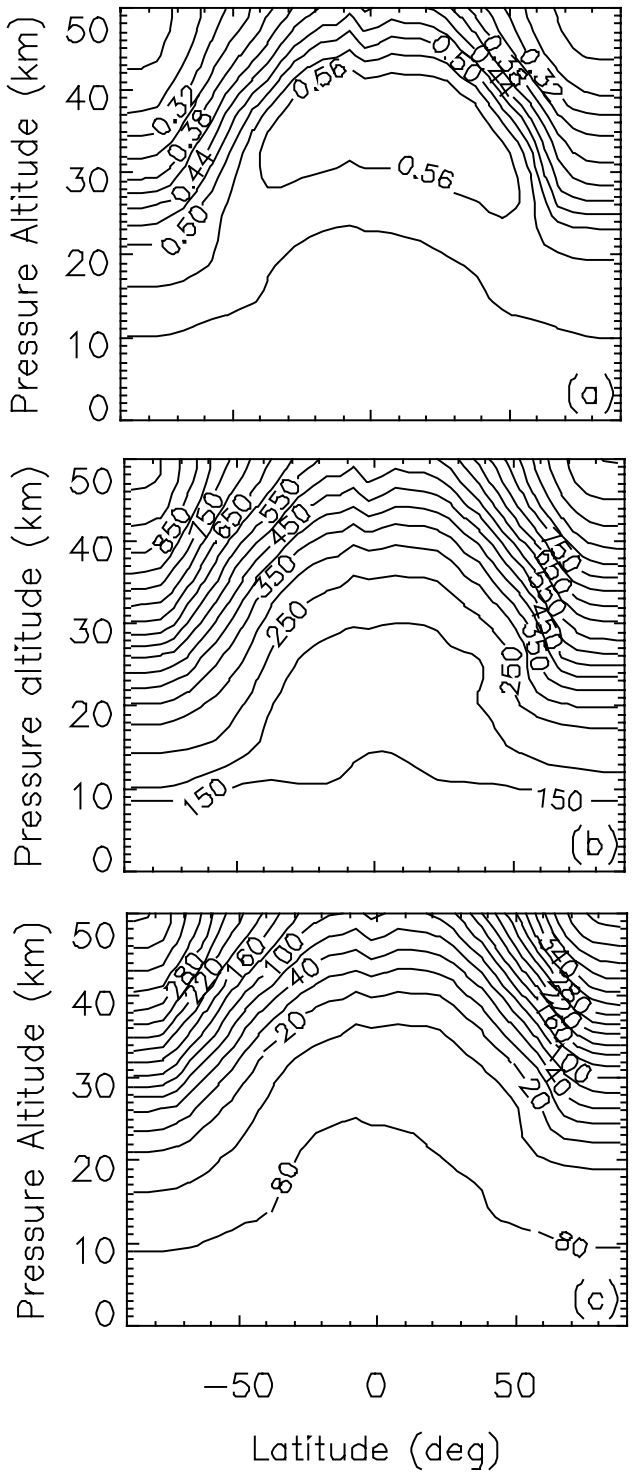

Figure 2. (a) Annually averaged molecular hydrogen mixing ratios in ppmv (micromoles/mole) predicted by LOTUS; mixing ratios in the troposphere vary between 0.50 and 0.53 ppmv. (b) Annually averaged deuterium isotopic composition of H_2 (‰ relative to VSMOW) predicted by S10. (c) Annually averaged deuterium isotopic composition of CH_4 (‰ relative to VSMOW) predicted by all model scenarios that use the *DeMore* [1993] CH_4 + OH KIE.

$\alpha'_{CH4\rightarrow H2}$, but also on the isotopic composition of the starting methane, a distinction that is important for the stratosphere.

[27] Modeled $\alpha'_{CH4\rightarrow H2}$ and $\delta D_{h\nu}$ reach steady values after about one year and are insensitive to the initial concentrations of HA and HB. As a check on our computational method, we find that $\delta D_{h\nu}$ calculated using HA and HB is, in most regions of the atmosphere, equivalent to the isotopic composition of formaldehyde, δD-CH_2O, predicted by S1–S3 and S9. The equivalence between $\delta D_{h\nu}$ and δD-CH_2O is expected because these scenarios have no IEs or KIEs in CH_2O photolysis or oxidation; the mostly small perturbations to this equivalence are due to the minor channel (R3) (CH_4 + $O(^1D)\rightarrow CH_2O$ + H_2), with larger perturbations at altitudes greater than ~40 km which we attribute to increasing $O(^1D)$ concentrations in the upper stratosphere (e.g., δD-CH_2O is greater than $\delta D_{h\nu}$ by up to ~200‰ at 60 km for S9).

[28] From these "instantaneous" grid cell calculations of $\alpha'_{CH4\rightarrow H2}$ and $\delta D_{h\nu}$, we then calculate monthly and annual averages for each grid cell, as well as additional averages for the stratosphere and troposphere (with the model tropopause determined as noted in section 2 and the model stratopause defined on the basis of climatological zonal temperature) weighted by mass or by the CH_4 oxidation rate, which we will use to broadly assess the sensitivities of $\alpha'_{CH4\rightarrow H2}$ and $\delta D_{h\nu}$ to isotope effects in H_2 production that may vary significantly with latitude and altitude. The annually averaged values weighted by mass or by CH_4 oxidation rate are obtained by averaging over latitude and altitude over the last 12 months of model integration and weighting the value by the total pressure or the CH_4 oxidation rate in each grid cell, respectively; in both calculations the difference in total mass in each grid cell at high versus low latitudes is accounted for by weighting by the integral of the cosine of latitude over the latitude range for each grid cell. Any sensitivity of averaged $\delta D_{h\nu}$ to weighting by CH_4 oxidation rate rather than by mass may be of interest in the troposphere where transport and mixing rates are rapid compared to the CH_4 and H_2 lifetimes.

3. Results and Discussion

[29] A contour plot of the annually averaged H_2 mixing ratio predicted by the LLNL 2-D model is shown in Figure 2a. In the lower stratosphere, the roughly constant mixing ratio of ~0.5 ppm reflects the approximate balance of H_2 production (from CH_4 oxidation) and loss (from H_2 oxidation). For air at higher latitudes and altitudes in the model, H_2 mixing ratios are lower because of higher OH, Cl and $O(^1D)$ mixing ratios and lower CH_4 mixing ratios in these regions, which lead to faster H_2 loss and slower H_2 production, respectively. Figure 2b shows annually averaged δD-H_2 predicted by the model for the composite scenario S10 as a function of latitude and altitude. As expected from the observations and box model studies, the 2-D model results show δD-H_2 increasing in the stratosphere as the air photochemically ages. Predicted values for δD-H_2 are greater than 800‰ for the oldest air at high latitudes and altitudes, which is extremely heavy compared to the average tropospheric value of 130‰. For comparison, Figure 2c shows contours of annually averaged

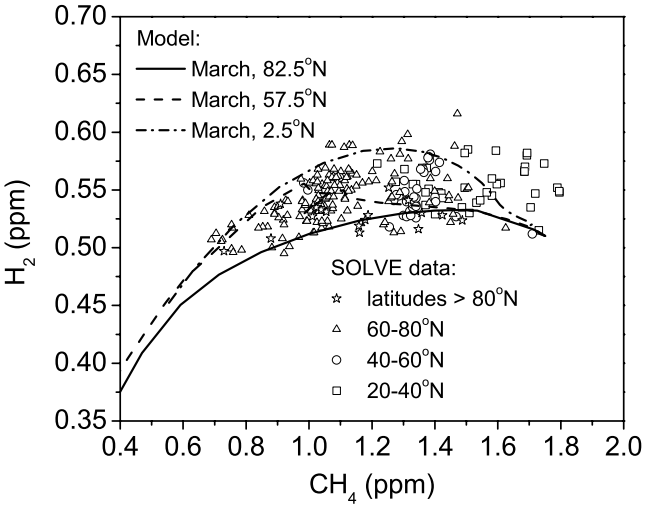

Figure 3. H_2:CH_4 relationships predicted by LOTUS in March as a function of latitude compared to H_2:CH_4 observations by the Airborne Chromatograph for Atmospheric Trace Species (ACATS-IV) during the SOLVE campaign (December 1999 to March 2000).

δD-CH_4 predicted by all model scenarios that use the *DeMore* [1993] CH_4 + OH KIE. As CH_4 is oxidized in the stratosphere, the KIEs for CH_4 + OH, Cl, and $O(^1D)$ enrich the remaining CH_4 in deuterium, with predicted values greater than 300‰ for the oldest air at high latitudes and altitudes. Since the stratospheric CH_4 reservoir from which H_2 is produced becomes more enriched in deuterium as the air photochemically ages, this enrichment is passed on to H_2, as noted by *Rahn et al.* [2003], unlike the troposphere where δD-CH_4 values remain close to −90‰.

[30] To make meaningful comparisons between the model results and the highly spatially resolved aircraft and balloon observations, we plot the quantities of interest as a function of methane mixing ratio rather than on a latitude-altitude plot. Latitude and altitude are not conserved quantities in the stratosphere, and this fact often leads to large variations in mixing ratios and isotopic compositions measured with high spatial resolution at a fixed location due to the complexity of stratospheric transport. Most of the variability is reduced by plotting the mixing ratio or isotopic composition versus another long-lived tracer such as CH_4 [see, e.g., *Plumb and Ko*, 1992; *Waugh et al.*, 1997].

[31] Modeled versus measured H_2:CH_4 relationships are shown in Figure 3. The H_2 and CH_4 mixing ratios shown here [*Herman et al.*, 2002, and references therein] were measured in situ aboard the ER-2 aircraft during the 1999–2000 NASA SOLVE campaign [*Newman et al.*, 2002] by the Airborne Chromatograph for Atmospheric Trace Species (ACATS-IV) instrument [*Elkins et al.*, 1996; *Romashkin et al.*, 2001] on the same flights that the whole air samples used for the δD-H_2 and CH_4 mixing ratio measurements from *Rahn et al.* [2003] (shown in later figures) were collected. The estimated precision and accuracy are 8% and 10%, respectively, for H_2 and 0.5% and 2.5%, respectively, for CH_4 [*Romashkin et al.*, 2001]. While Figure 3 shows model results for the month of March, we note that maximum seasonal differences in predicted H_2 mixing ratios are ∼0.01 ppmv for CH_4 mixing ratios >0.8 ppm and ∼0.05 ppmv for CH_4 between 0.4 and 0.8 ppmv. Although the H_2 observations show significant scatter, Figure 3 illustrates that the model results effectively capture the observed H_2:CH_4 relationships and their trend with latitude. Similarly, the chemistry and transport in the model simulate the observed δD-CH_4:CH_4 relationships sufficiently well [see *McCarthy et al.*, 2003, Figure 12] to use the model to investigate the sensitivity of δD-H_2 and $\delta D_{h\nu}$ to various known and unknown isotope effects in the production of H_2 from CH_4 oxidation.

[32] Modeled versus measured δD-H_2:CH_4 relationships for the stratosphere from selected scenarios are shown in Figures 4 and 5. Model results in Figures 4 and 5 (lines) are for March at 82.5°N since the lowest CH_4 mixing ratio samples were collected in March at 80°N. However, predicted δD-H_2 for a given CH_4 mixing ratio varies by less than 20‰ (<30‰ for scenarios 5–8) for all latitudes and months, as indicated by the envelopes of all model results for several scenarios in Figure 5 (gray-shaded regions). Observations of stratospheric δD-H_2 obtained from a balloon flight at 40°N in October 2002 [*Röckmann et al.*, 2003] are also plotted in Figure 5 and exhibit a similar δD-H_2:CH_4 relationship to the ER-2 data but with an offset of up to ∼50‰ at lower CH_4 mixing ratios. The measurement discrepancies cannot be explained as meridional or seasonal differences in the δD-H_2:CH_4 relationships, at least as simulated by the model, since the measurement differences exceed the total variability expected in the stratosphere on the basis of the model results for all scenarios in this study and since modeled H_2 for a given CH_4 mixing ratio tends to be isotopically lighter at lower latitudes than at high latitudes, which is the opposite trend with latitude between the two data sets. Since laboratory intercomparisons of δD-H_2 measurements have yet to be made, and since large uncertainties in the isotope effects and branching ratios in the production of H_2 from CH_4 oxidation lead to a range of predicted δD-H_2 values that greatly exceeds the difference between the two data sets, for simplicity we will focus our sensitivity discussion below on intercomparisons between the ER-2 measurements and the model results.

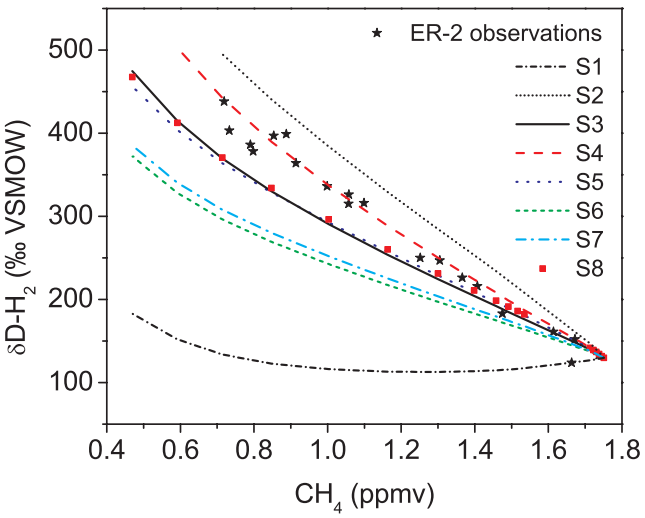

Figure 4. δD-H_2 plotted as a function of CH_4 mixing ratio for various scenarios (see Table 4) for March at 82.5°N. ER-2 observations are plotted as stars.

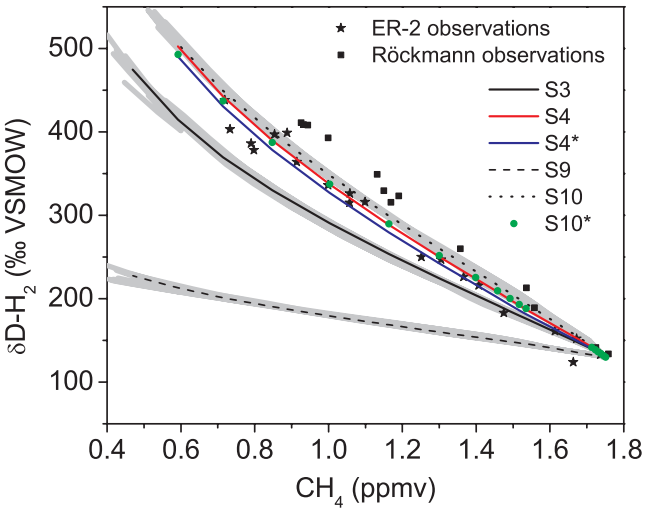

Figure 5. δD-H_2 plotted as a function of CH_4 mixing ratio for various scenarios (see Table 4). The ER-2 observations are plotted as stars, and the Röckmann balloon observations [*Röckmann et al.*, 2003] are plotted as squares. Gray shading represents the envelopes of model results for all latitudes and seasons for S3, S9 and S10.

However, none of our discussion or conclusions depends on which data set shown in Figure 5 is used. We also note that observations of δD-H_2 from an additional balloon flight are reported by *Rhee et al.* [2006b, see Figure 2] and that these new data generally fall between the ER-2 and the *Röckmann et al.* [2003] observations.

3.1. Sensitivity of Stratospheric δD-H_2 to H Atom Abstraction Branching Ratios and Kinetic and Photolysis Isotope Effects

[33] The sensitivity of modeled δD-H_2 in the stratosphere to magnitudes of the branching ratios for H versus D abstraction along the oxidation pathway from CH_3D to HD is shown in Figure 4. As discussed in section 2.1, S1 and S2 represent the minimum and maximum deuterium retention in the product H_2, respectively, based on the use of statistical and maximum branching ratios for (R1), (R2), (R3), and (R9), and the difference in modeled δD-H_2 is large: ~350‰ at 0.8 ppmv of CH_4. Values of δD-H_2 for S3, with more realistic but still underconstrained branching ratios, are intermediate between these extremes. In addition, we find that the branching ratios for the CH_3D + oxidant reactions ((R1)–(R3)) and for the $CH_2DO + O_2$ reaction (R9) are both likely important in the deuterium enrichment of H_2, on the basis of several simulations (not shown) in which branching ratios for (R1), (R2) and (R3) were set to their S3 values and the (R9) branching ratio was statistical and vice versa; because (R2) and (R3) are minor channels of the $CH_4 + O(^1D)$ reaction, we conclude that (R1) and (R9) are likely to be of approximately equal importance in determining the deuterium enrichment in stratospheric H_2. In short, our simulations demonstrate that branching ratios likely play a very large role in enriching stratospheric H_2 in deuterium, as first suggested by *Gerst and Quay* [2001], and that accurate measurements and/or theoretical predictions are needed to better constrain the absolute and relative magnitudes of their effects on δD-H_2.

[34] The sensitivity of modeled δD-H_2 in the stratosphere to KIEs in the oxidation of formaldehyde by OH, Cl, Br, and $O(^3P)$ is shown in Figure 4 by scenarios S3 and S4. In S3, recall that all formaldehyde oxidation KIEs are set to 1. In S4, we use S3 branching ratios but also include the experimentally determined CH_2O oxidation KIEs. The resulting δD-H_2 is almost 100‰ heavier than S3 for CH_4 mixing ratios less than 0.8 ppmv, indicating that KIEs in the oxidation of formaldehyde are indeed an important factor in enriching H_2 in deuterium.

[35] The sensitivity of modeled δD-H_2 in the stratosphere to possible isotope effects in formaldehyde photolysis are illustrated by scenario results plotted in Figures 4 and 5. In S5, recall that both the value for J_{R11a}/J_{R11b} determined by *Crounse et al.* [2003] at the surface and the relative photolysis rate coefficient ratio measured at the surface by Nielsen and coworkers (i.e., $(J_{R11a} + J_{R12a})/(J_{R11b} + J_{R12b}) = 1.44$) are used. Interestingly, the photolysis IEs in S5 result in stratospheric δD-H_2 values that are very similar to those predicted by S3 without photolysis IEs (in Figure 4, δD-H_2 for S5 is greater than that for S3 by ~5‰ at 1.4 ppm CH_4 and smaller than that for S3 by ~10‰ at 0.6 ppm CH_4 at 82.5°N). Results for S10 (with CH_2O oxidation KIEs and photolysis IEs) and S4 (with CH_2O oxidation KIEs but without photolysis IEs) are also very similar to each other (Figure 5). These similarities show that the constraints on photolysis IEs determined at the surface by Crounse et al. and Nielsen et al. that result in isotopically lighter H_2 than the starting CH_2O and a slower photolysis rate for CHDO than for CH_2O, respectively, do not result in significantly lighter δD-H_2 values in the stratosphere when these particular surface constraints are applied globally in the model. Furthermore, these surface constraints lead to significantly larger, not smaller or similar, values for $\delta D_{h\nu}$ in the stratosphere, as shown in section 3.2 below. In contrast, S6, which is also consistent with the relative photolysis rate coefficient ratio of Nielsen and coworkers but which has an arbitrarily smaller radical channel IE (J_{R12a}/J_{R12b}) and larger molecular channel IE (J_{R11a}/J_{R11b}) than S5, results in stratospheric H_2 that is significantly lighter than that predicted by S5 (S6 is lighter than S5 by ~75‰ at 0.6 ppmv CH_4). In general, comparison of the results from S3, S5 and S6 illustrates the sensitivity of stratospheric δD-H_2 to the two competing formaldehyde photolysis IEs on stratospheric δD-H_2: a molecular channel IE results in faster production of H_2 than HD (and thus lighter values of δD-H_2 would be expected than in the absence of a molecular channel IE), but at the same time a radical channel IE enriches formaldehyde in deuterium without forming H_2 or HD, making the H_2 produced by the competing molecular channel heavier than in the absence of a radical channel IE. Thus these sensitivity runs suggest that the larger (smaller) the radical channel IE is relative to the molecular channel IE, the isotopically heavier (lighter) is the resulting H_2.

[36] The sensitivity of stratospheric δD-H_2 to a possible wavelength dependence for the underlying formaldehyde photolysis IEs was investigated with S7 and S8 (Figure 4) and S7a and S8a (not shown). S7 and S7a (for which the globally averaged photolysis IEs from S7 were used) yielded virtually identical δD-H_2:CH_4 relationships (not

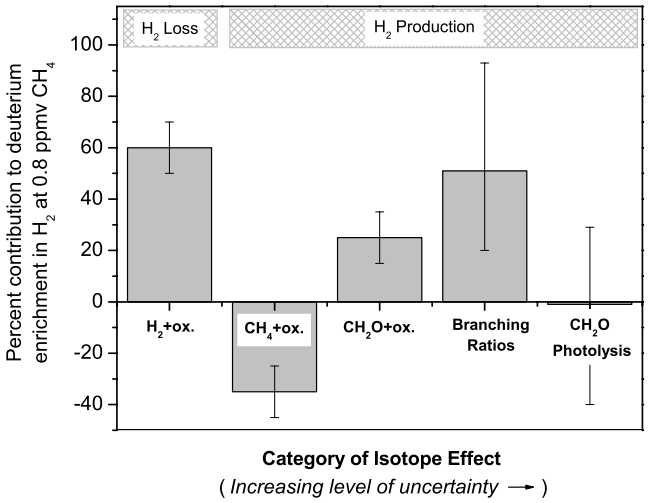

Figure 6. Percent contributions to deuterium enrichment in stratospheric H_2 at a CH_4 mixing ratio of 0.8 ppmv estimated from model sensitivities for each category of isotope effect, with level of uncertainty increasing to the right (see text in section 2.6 for details).

shown), as did S8 and S8a (for which the globally averaged photolysis IEs from S8 were used; not shown). These results indicate that stratospheric δD-H_2 is not particularly sensitive to hypothetical wavelength dependences of the underlying CH_2O photolysis IEs, at least as we have formulated them here. Rather, the results for S7, S7a, S8, and S8a further illustrate our generalization above that stratospheric δD-H_2 is sensitive to the average relative magnitudes of the molecular and radical channel IEs. For example, S7 yields a δD-H_2:CH_4 relationship that is similar to but heavier by $\sim$10‰ than that for S6, consistent with the fact that the average magnitude of the molecular channel IE in S7 is similar to that in S6 while that for the radical channel IE in S7 is larger than in S6 (see Table 5). Furthermore, S8, in which the CHDO absorption cross sections and quantum yields are blue-shifted with respect to CH_2O, yields a δD-H_2:CH_4 relationship that is nearly identical to that for S5 (for all model altitudes and seasons). This similarity can be explained by the fact that, although the absolute magnitudes of the photolysis IEs in S5 and S8 are different, in both S5 and S8 the radical channel IE is approximately 4 times greater than the molecular channel IE. Thus these results suggest that the sensitivity of stratospheric δD-H_2 to photolysis IEs is controlled primarily by the average relative magnitudes of the molecular and radical channel IEs (i.e., the values for $(J_{R11a}/J_{R11b})_{avg}$ and $(J_{R12a}/J_{R12b})_{avg}$) rather than by an explicit wavelength dependence for the IEs that we tested. Importantly, however, the insensitivity of modeled δD-H_2 in the stratosphere to wavelength-dependent versus wavelength-independent photolysis IEs does not necessarily hold true for $\alpha'_{CH4\rightarrow H2}$ and $\delta D_{h\nu}$, as we discuss in section 3.2 below. In summary, our sensitivity runs show that, while stratospheric δD-H_2 is sensitive to varying degrees to the underlying formaldehyde photolysis IEs (depending on how we formulated them), the range of possibilities in terms of both the magnitudes and characteristics of the IEs themselves, how these may vary in different regions of the atmosphere, and the magnitude of their effect on δD-H_2 is large and cannot yet be unambiguously constrained by measurements of the ratios of J-values at the surface of the type made by *Crounse et al.* [2003] and Nielsen and coworkers, by the stratospheric δD-H_2 observations, nor a combination of the two.

[37] The sensitivity of stratospheric δD-H_2 to KIEs in the H_2 loss reactions and the CH_4 + OH reaction are shown in Figure 5. In the absence of KIEs for H_2 + OH and H_2 + Cl (S9), values for δD-H_2 are lower than those for S3 (which include these KIEs) by $\sim$150‰ at a methane mixing ratio of 0.8 ppmv. Clearly, KIEs in the oxidation of H_2 are a major factor in the extreme deuterium enrichment in stratospheric H_2 above its tropospheric value, as first shown by *Rahn et al.* [2003], accounting for $\sim$60% of the enrichment in the model scenarios run here. Varying the H_2 + OH KIE within the limits of the reported experimental uncertainty results in changes in predicted δD-H_2 of $\sim$15‰ (not shown), significantly less than the range of modeled δD-H_2 due to choices for branching ratios and on the order of the δD-H_2 measurement precision. We also find that modeled δD-H_2 is insensitive to changing the magnitude of the H_2 + Cl KIE by $\sim$50%, which is the difference between the experimental determinations of *Taatjes* [1999] and *Persky and Klein* [1966] noted in section 2.4. To illustrate the sensitivity to the CH_4 + OH KIE, results for S4* and S10* using the *Gierczak et al.* [1997] CH_4 + OH KIE are also shown in Figure 5, revealing slightly lower values for δD-H_2 of up to 10‰ at CH_4 mixing ratios of $\sim$0.9 to 1.1 ppmv than from those from S4 and S10 using the *DeMore* [1993] CH_4 + OH KIE. Thus stratospheric δD-H_2 is not very sensitive to the difference between the KIEs reported by these two laboratories.

[38] Finally, as for a mesospheric influence on stratospheric δD-H_2 due to the photolysis of mesospheric water vapor and transport to the stratosphere, our simulations with values for δD-H_2 of -200‰ (between 75 and 85 km in the mesosphere) and -800‰ (at the top of the model between 83.5 and 85 km) showed a decrease of about $\sim$20‰ and $\sim$10‰, respectively, in stratospheric δD-H_2 at a methane mixing ratio 0.8 ppmv. This difference decreased with increasing methane mixing ratios and was negligible for $CH_4 > 1.4$ ppm. We conclude that, for well-mixed air (i.e., for air not perturbed by filaments of mesospheric air), H_2 produced in the mesosphere from water photolysis will have a small (<20‰) to negligible effect on ''background'' stratospheric δD-H_2 values. However, these sensitivity runs also suggest that details of mesosphere-to-stratosphere transport during the polar winter of 1999–2000 not captured by LOTUS [see, e.g., *Plumb et al.*, 2003] could potentially explain at least part of the difference between the *Rahn et al.* [2003] ER-2 aircraft data and the *Röckmann et al.* [2003] balloon data, with lighter δD-H_2 values observed at high latitudes in winter (ER-2) than at midlatitudes in October (balloon), and warrant further analysis.

[39] In summary, our results and analyses above suggest that branching ratios along the pathway from CH_3D to HD and H_2, KIEs for formaldehyde oxidation, IEs in formaldehyde photolysis, and KIEs for H_2 oxidation all play or, in the case of formaldehyde photolysis IEs, have the potential to play a significant role in determining the isotopic composition of stratospheric H_2. Summarizing the results of our sensitivity study here, Figure 6 illustrates our best

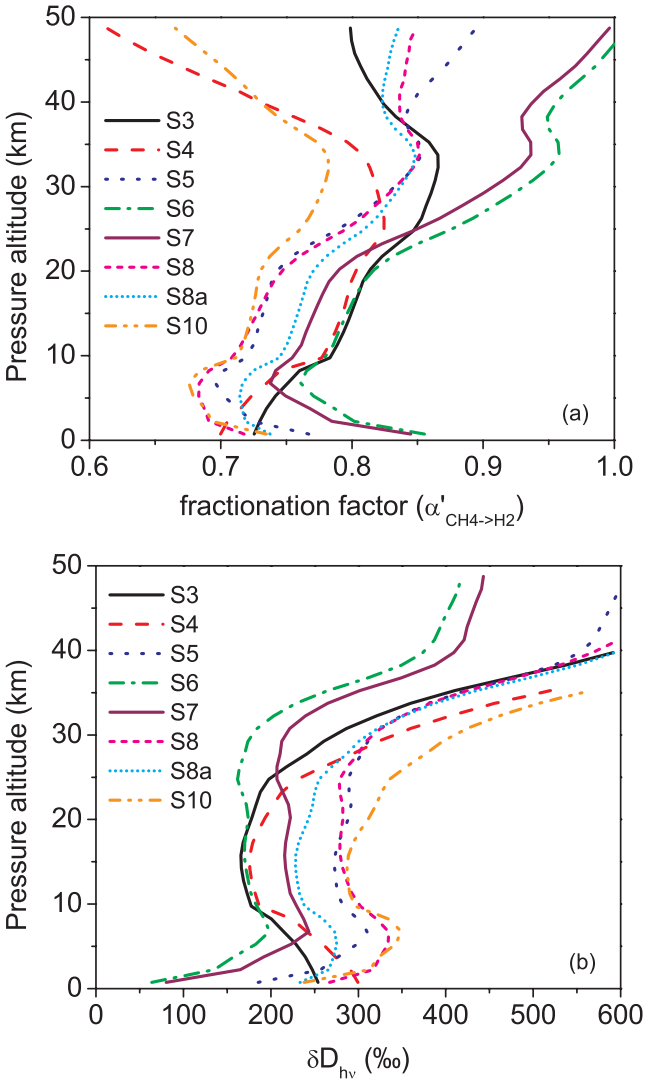

Figure 7. Annually averaged (a) $\alpha'_{CH4\rightarrow H2}$ and (b) $\delta D_{h\nu}$ (‰ versus VSMOW) plotted as a function of altitude for S3, S4, S5, S6, S7, S8, S8a and S10 at 82.5°N.

estimates of the percent contribution of each of these categories of isotope effects to deuterium enrichment in stratospheric H_2 at a CH_4 mixing ratio of 0.8 ppmv. Note that the uncertainties in the percent contributions of the CH_3D branching ratios and the CH_2O photolysis isotope effects, the 2 classes of isotope effects in the individual reaction steps for the oxidation of CH_4 to H_2 that we currently know the least about, are large and interrelated (see section 2.6), and thus their representation in Figure 6 should be considered as a rough guide providing qualitative insight until additional information on one or both of these isotope effects becomes available. Furthermore, our sensitivity runs also demonstrate that very similar δD-H_2:CH_4 relationships in the stratosphere can result from very different choices for isotope effects, particularly for the (R1)–(R3) and (R9) branching ratios and CH_2O photolysis isotope effects and, thus, that stratospheric observations cannot yet be used to accurately quantify these isotope effects individually. Importantly, however, as we discuss in the following 2 sections, different isotope effects for individual reactions that result in similar stratospheric δD-H_2:CH_4 relationships can result in very different values for $\delta D_{h\nu}$ in the troposphere, a point with important implications for determination of an accurate average value for $\delta D_{h\nu}$ in the troposphere for use in the global H_2 isotope budget and a further caveat that our estimates in Figure 6 are applicable to stratospheric H_2 near CH_4 mixing ratios of 0.8 ppmv (or a stratospheric mean age of ~5 years [*Andrews et al.*, 2001]).

3.2. Modeled $\alpha'_{CH4\rightarrow H2}$ and $\delta D_{h\nu}$ and Their Variation With Altitude and Latitude

[40] Annually averaged altitude profiles of modeled $\alpha'_{CH4\rightarrow H2}$ and $\delta D_{h\nu}$ are shown in Figure 7 for selected scenarios at 82.5°N, while annually averaged latitude-altitude contour plots are shown in Figures 8 ($\alpha'_{CH4\rightarrow H2}$) and 9 ($\delta D_{h\nu}$). Clearly, there are large variations in $\alpha'_{CH4\rightarrow H2}$ and $\delta D_{h\nu}$ with respect to latitude and altitude and between different scenarios, even for scenarios which yielded very similar δD-H_2:CH_4 relationships in the stratosphere. In this section, we discuss these variations and the underlying processes that control them in each of the different scenarios. While annually averaged values are presented, we note that the seasonal variation in $\alpha'_{CH4\rightarrow H2}$ is negligible in the troposphere, that $\alpha'_{CH4\rightarrow H2}$ can vary seasonally by up to a factor of two above 15 km (due to seasonal variations in the fraction of CH_4 oxidized by OH, $O(^1D)$, and Cl), and that the seasonal variation in $\delta D_{h\nu}$ is less than 20‰ at all latitudes and altitudes (despite variations in stratospheric $\alpha'_{CH4\rightarrow H2}$ since the corresponding seasonal variations in δD-CH_4 act to oppose those in $\alpha'_{CH4\rightarrow H2}$).

[41] In the troposphere, the shapes of the altitude profiles of $\alpha'_{CH4\rightarrow H2}$ and $\delta D_{h\nu}$ for any given scenario are like mirror images of each other, demonstrating that the processes that determine overall values for $\alpha'_{CH4\rightarrow H2}$ also control the variations in $\delta D_{h\nu}$ with altitude there. For S3 and S4, which do not include CH_2O photolysis IEs, the trends with altitude in the troposphere are controlled primarily by the temperature dependence of the CH_4 + OH KIE, as is clear from comparing S3 and S4 with S3** in which the CH_4 + oxidant KIEs were set to 1 (Figure 10). This temperature dependence results in H_2 that is isotopically lighter at the lower temperatures in the upper troposphere than at the higher temperatures at the surface. The magnitudes of $\alpha'_{CH4\rightarrow H2}$ and $\delta D_{h\nu}$ for S3 and S4, however, are different since S4 includes the KIEs for CH_2O oxidation, resulting in values of $\delta D_{h\nu}$ for S4 that are heavier by 10 to 50‰ than those for S3 at 82.5°N. In the stratosphere, changes in $\delta D_{h\nu}$ with altitude no longer mirror changes in $\alpha'_{CH4\rightarrow H2}$: values for $\delta D_{h\nu}$ increase dramatically for all scenarios in the middle and upper stratosphere as the stratospheric CH_4 reservoir becomes increasingly enriched, while trends in $\alpha'_{CH4\rightarrow H2}$ with altitude are more complex and depend on the scenario. For S3 (and to a lesser extent S5, S8, and S8a), the stratospheric trend in $\alpha'_{CH4\rightarrow H2}$ with altitude is dominated by the changing fractions of CH_4 oxidized by OH, $O(^1D)$, and Cl. For example, below 35 km the fraction of CH_4 oxidized by Cl generally increases in the stratosphere, resulting in an increase in $\alpha'_{CH4\rightarrow H2}$ with altitude since the CH_4 + Cl KIE is larger than that for CH_4 + OH. Above 35 km, the rate of CH_4 oxidation by $O(^1D)$ increases substantially, which then reverses or attenuates this increase

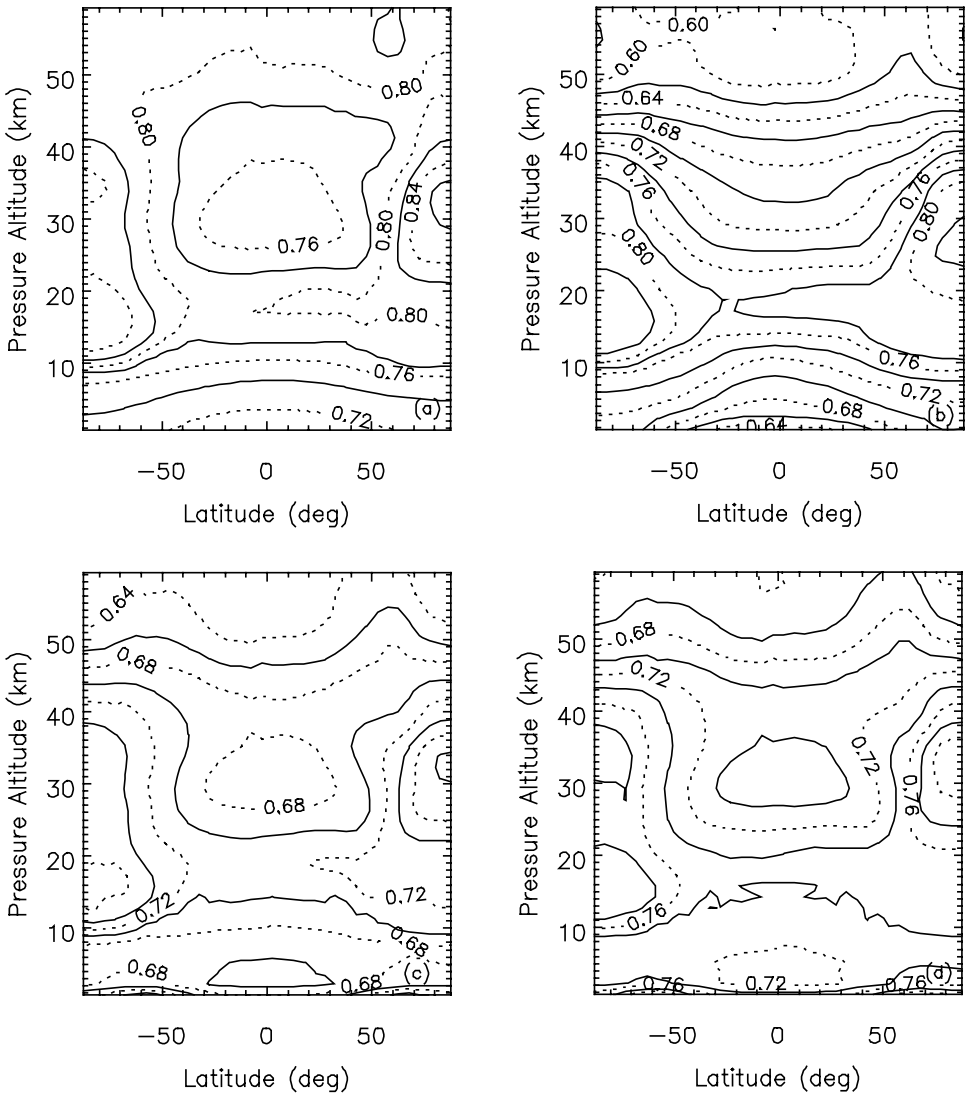

Figure 8. Annually averaged $\alpha'_{CH4\rightarrow H2}$ plotted as a function of latitude and altitude for (a) S3, (b) S4, (c) S10, and (d) S10*. Contours are plotted at intervals of 0.02.

(since the $CH_4 + O(^1D)$ KIE is smaller than both the KIEs for CH_4 + OH and CH_4 + Cl) depending on what other IEs are competing in the various scenarios. For scenarios that also include CH_2O oxidation KIEs (S4 and S10), both the increasing fraction of CH_2O oxidized versus photolyzed and the changing fractions of CH_2O oxidized by OH, Cl, Br and $O(^3P)$ also play a major role in determining values for $\alpha'_{CH4\rightarrow H2}$ and $\delta D_{h\nu}$ and their trend with altitude, particularly the sharp decrease in $\alpha'_{CH4\rightarrow H2}$ above ~35 km due to the increased fraction and rate of CH_2O oxidized by Br with an exceptionally large KIE of 3.27.

[42] The scenarios with CH_2O photolysis IEs yield interesting sensitivities. The trends with altitude for $\alpha'_{CH4\rightarrow H2}$ and $\delta D_{h\nu}$ for scenarios with CH_2O photolysis IEs (S5–S8) are generally the opposite of those without photolysis IEs (S3, S4), with $\alpha'_{CH4\rightarrow H2}$ and $\delta D_{h\nu}$ decreasing and increasing with altitude, respectively, in the troposphere and roughly the opposite trends for $\alpha'_{CH4\rightarrow H2}$ in the stratosphere (except between ~10 and 20 km where they are similar). A steady state analysis of the $[CH_2O]/[CHDO]$ ratio using model output for J_{11a}, J_{12a}, and ($k_{CH2O+OH}[OH] + k_{CH2O+Cl}[Cl] + k_{CH2O+Br}[Br] + k_{CH2O+O}[O(^3P)]$) shows that, when the trends in the scenarios with photolysis IEs differ from those without photolysis IEs, they are largely controlled by steady state changes in the $[CH_2O]/[CHDO]$ ratio due to the changing fractions of formaldehyde destroyed by (R10), (R11), and (R12). Thus, although the fraction of CH_2O destroyed by photolysis to the molecular channel (f_{molec}) increases steadily with altitude in the troposphere (e.g., at 82.5°N, f_{molec} = 0.60, f_{rad} = 0.24, and f_{oxid} = 0.16 at the surface versus f_{molec} = 0.72, f_{rad} = 0.25, and f_{oxid} = 0.03 at 10 km, a result of the fact that J_{R11a} increases by a factor of ~14, J_{R12a} increases by a factor of ~12 and $k_{total}[OX]$ increases by a factor of ~2 from the surface to 10 km), the combination of the dramatically decreasing fraction oxidized (f_{oxid}) and the small increasing fraction photolyzed to the radical channel (f_{rad}) results in isotopically heavier formaldehyde at steady state with altitude in the troposphere, which in turn results in the trend of smaller $\alpha'_{CH4\rightarrow H2}$ (larger $\delta D_{h\nu}$) with altitude. In the troposphere,

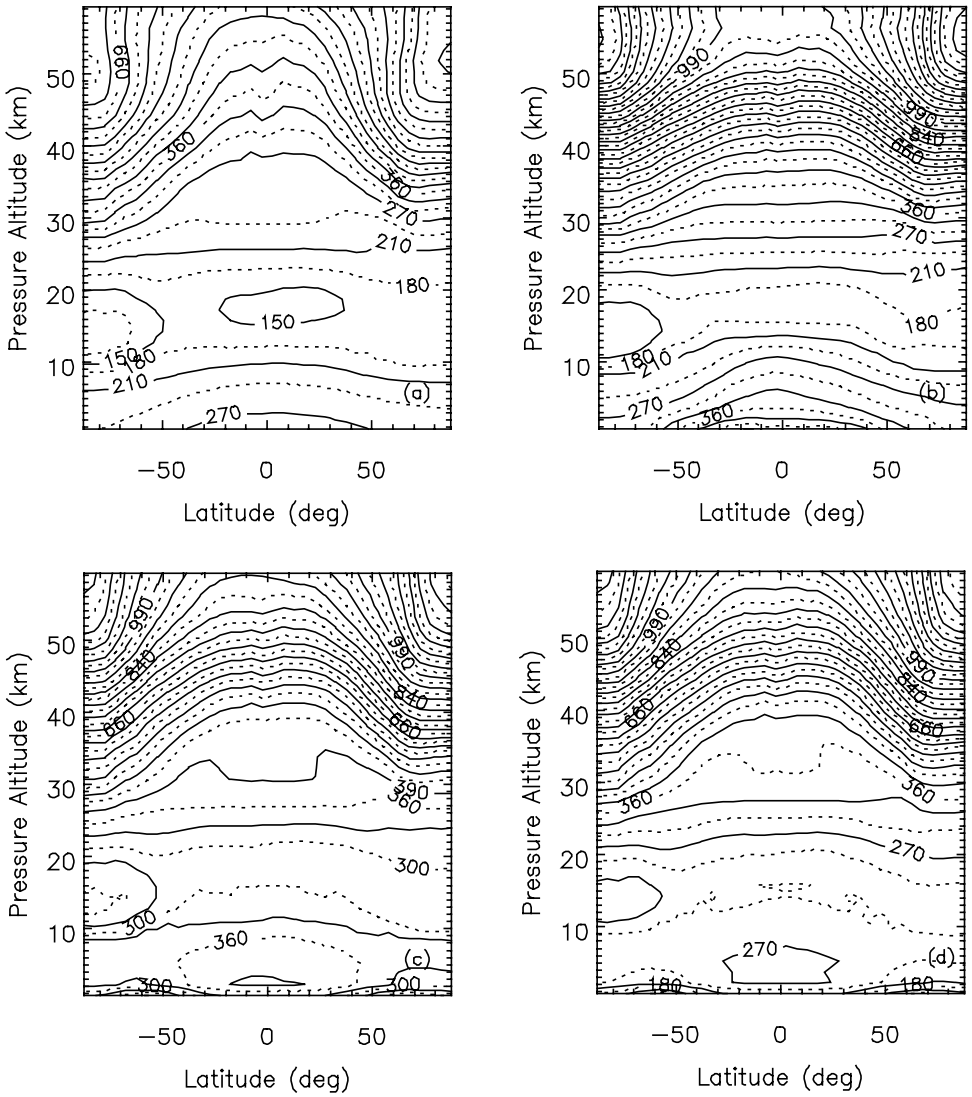

Figure 9. Annually averaged $\delta D_{h\nu}$ in ‰ versus VSMOW plotted as a function of latitude and altitude for (a) S3, (b) S4, (c) S10, and (d) S10*. Contours are plotted at 30‰ intervals.

this effect competes with the temperature dependence of the CH_4 + OH KIE, which reverses the increasing trend in $\delta D_{h\nu}$ with altitude in the upper troposphere where temperatures are the coldest for scenarios that include CH_2O photolysis IEs, as illustrated by comparing trends in S5 (with photolysis IEs) and S5** (with photolysis IEs but with all CH_4 + oxidant KIEs set to 1) in Figure 10. In the stratosphere, the opposite trend with altitude in the fractions of formaldehyde destroyed by oxidation and photolysis to the molecular and radical channels is largely responsible for the stratospheric trends in $\alpha'_{CH4\rightarrow H2}$ above ~20 km for S5–S8, while $\delta D_{h\nu}$ above 20 km is additionally influenced by the increasing deuterium enrichment in the CH_4 reservoir, as discussed above.

[43] The simple steady state analysis above yields insight into the processes controlling the trends in $\alpha'_{CH4\rightarrow H2}$ and $\delta D_{h\nu}$ with altitude in a given scenario. However, the actual values for $\alpha'_{CH4\rightarrow H2}$ and $\delta D_{h\nu}$ also depend, of course, on the relative and absolute magnitudes of the photolysis IEs, just as discussed for δD-H_2. For example, the radical channel IE in S5 is larger than that in S6, which results in values for $\delta D_{h\nu}$ at the surface that are ~120 ‰ heavier for S5 than for S6, while the shapes of the altitude profiles for $\delta D_{h\nu}$ are virtually identical for both scenarios. A similar argument explains why S7a (not shown but virtually identical to S7) yields values for $\delta D_{h\nu}$ that are ~40 ‰ heavier than S6. The combined results from S7, S7a, S8, and S8a also suggest that a potential dependence of the relative quantum yields and/or the relative absorption cross sections for CH_2O versus CHDO photolysis on actinic flux (i.e., wavelength) may or may not result in significant differences in $\alpha'_{CH4\rightarrow H2}$ and $\delta D_{h\nu}$ depending on whether or not the wavelength dependence results in large differences in the relative magnitudes of the molecular versus radical channel J-values in different regions of the atmosphere relative to the globally averaged values. For example, results for S7 and S7a (not shown) are nearly identical (with maximum differences in $\delta D_{h\nu}$ of <10‰ above 40 km), suggesting little effect of the wavelength dependence of the quantum yields as formulated in S7. However, S8 and S8a yield signifi-

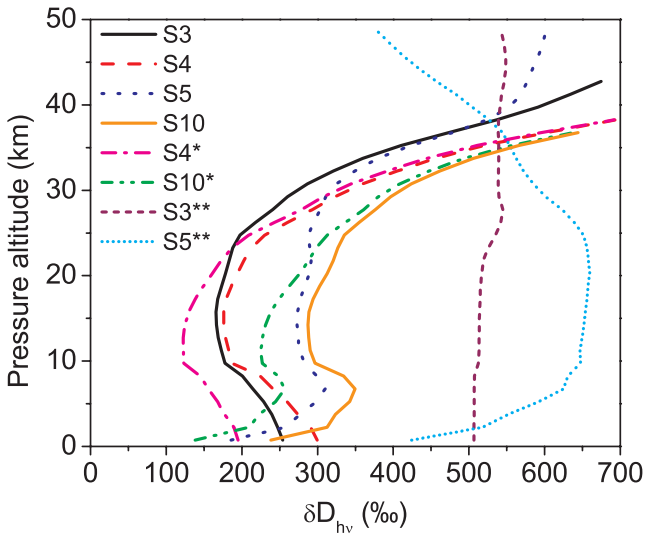

Figure 10. Annually averaged $\delta D_{h\nu}$ (‰ versus VSMOW) plotted as a function of altitude for S3, S4, S5, S10, S4*, S10*, S3** and S5** at 82.5°N.

cantly different profiles for $\alpha'_{CH4\rightarrow H2}$ and $\delta D_{h\nu}$ from one another, which can be explained by the fact that the particular blue-shifted cross sections and quantum yields in S8 result in ranges of values for J_{R11a}/J_{R11b} and J_{R12a}/J_{R12b} that are significantly greater than those in S7, especially J_{R12a}/J_{R12b} (see Table 5), and that values for J_{R11a}/J_{R11b} are smallest at the surface and generally increase with altitude while values for J_{R12a}/J_{R12b} are largest at the surface and generally decrease with altitude. This large radical channel IE (compared to the average IE for S8 calculated over the troposphere and stratosphere) in combination with a small molecular channel IE near the surface results in values for $\delta D_{h\nu}$ for S8 below 25 km that are ~75‰ heavier than for S8a, in which the globally averaged ratios of J-values from S8 are used. Thus, although stratospheric δD-H_2:CH_4 relationships were nearly identical for S8, S8a, and S5, values for $\alpha'_{CH4\rightarrow H2}$ and $\delta D_{h\nu}$ for these scenarios for the troposphere are quite different from one another.

[44] A comparison of results for S4 (CH_2O KIEs but no photolysis IEs) and S10 (CH_2O KIEs and surface-constrained photolysis IEs) is also informative. Similar to the combination of S8, S8a, and S5, these two scenarios yield very similar δD-H_2:CH_4 relationships to one another (and are both within ±40‰ of the ER-2 observations) yet very different values for $\alpha'_{CH4\rightarrow H2}$ and $\delta D_{h\nu}$, at least below 30 km. We believe these similarities in stratospheric δD-H_2 for scenarios with quite different $\alpha'_{CH4\rightarrow H2}$ and $\delta D_{h\nu}$ profiles likely result from the effects of stratospheric transport as well as the similarity of the magnitudes of $\alpha'_{CH4\rightarrow H2}$ above 25 km where stratospheric CH_4 oxidation rates reach a maximum. First, recall that values for $\alpha'_{CH4\rightarrow H2}$ and $\delta D_{h\nu}$ were specifically calculated so as not to include the effects of transport. As species are transported, however, differences between $\alpha'_{CH4\rightarrow H2}$ and $\delta D_{h\nu}$ in different grid cells will be attenuated. Indeed, when we ran model simulations allowing "HA" and "HB" to be transported, differences in $\delta D_{h\nu}$ between S5 and S8, for example, decreased significantly. Second, we note that values for $\alpha'_{CH4\rightarrow H2}$ are only part of what determines the influence of various isotope effects in CH_4 oxidation on the stratospheric δD-H_2:CH_4 relationships; the rate of CH_4 oxidation also matters. Thus the fact that the magnitudes of $\alpha'_{CH4\rightarrow H2}$ in each of these sets of scenarios are more or less similar at and above 25 km where CH_4 oxidation rates are highest likely also contributes to similar stratospheric δD-H_2:CH_4 relationships observed for, e.g., S4 and S10, despite significantly different values for $\alpha'_{CH4\rightarrow H2}$ at lower altitudes. These results caution against having confidence in the extrapolation of isotopic fractionation factors for the production of H_2 in the stratosphere to the troposphere based on good agreement with stratospheric observations, at least until additional information is available to better constrain the branching ratios, photolysis IEs, or both.

[45] A final comparison of $\alpha'_{CH4\rightarrow H2}$ and $\delta D_{h\nu}$ profiles from S4 and S10 (or S4* and S10*, all shown in Figure 10) yields a result for altitudes greater than ~2 km that at face value might at first seem surprising given the measurements at the surface. In the lowest model level (0–1.5 km), inclusion of the surface-constrained CH_2O photolysis IEs in S10 yields a value for $\delta D_{h\nu}$ of about ~235‰, lower by ~65‰ than the value of 300‰ from S4 without photolysis IEs. Thus inclusion of IEs in the photolysis of CH_2O using relative J-values determined at the surface in sunlight, all else being equal, yields isotopically lighter H_2 in this altitude range than not including photolysis IEs, in line with expectations from the surface measurements made by *Crounse et al.* [2003] and Nielsen and coworkers. However, at altitudes of 2 km and higher, inclusion of the photolysis IEs in S10 produces H_2 that is isotopically heavier than H_2 produced by S4 without photolysis IEs, the opposite of what might be expected to zeroth-order on the basis of the surface measurements alone. The result that inclusion of photolysis IEs in S10 yields isotopically lighter H_2 at the surface but isotopically heavier H_2 at all altitudes above 2 km is due to the relatively large radical channel IE compared to the molecular channel IE in S10 coupled with the large increase in J-values for CH_2O photolysis with altitude (and, importantly, the corresponding decrease in the fraction of CH_2O oxidized, as discussed above). A comparison of S3 (branching ratios only) and S5 (branching ratios + surface-constrained photolysis IEs) leads to a similar conclusion (but smaller values of $\delta D_{h\nu}$ overall since neither of these scenarios contains CH_2O oxidation KIEs). If the molecular channel IEs are changed to be relatively larger than the constraints on the molecular and radical channel IEs provided by the experiments of Crounse et al. and Nielsen and coworkers, then such CH_2O photolysis IEs can result in isotopically "neutral" or isotopically lighter H_2 compared to a scenario without the photolysis IEs (compare, e.g., S3 and S6) even at altitudes above the surface. Alternatively, a relatively larger radical channel IE could result in isotopically heavier H_2 everywhere and not just at altitudes above 2 km. Although the particular model results presented here are highly dependent on how we have formulated the underconstrained photolysis IEs, they do at least caution against making simple arguments as to how $\delta D_{h\nu}$ may vary in the troposphere and stratosphere on the basis of constraints on CH_2O photolysis isotope effects determined for conditions at Earth's surface without performing at least a

Table 7. Sensitivity of Values for $\alpha'_{CH4\rightarrow H2}$ and $\delta D_{h\nu}$ to Various Model Scenarios

	$\alpha'_{CH4\rightarrow H2}$ ($\alpha_{CH4\rightarrow H2}$) Weighted by Mass		$\delta D_{h\nu}$, ‰, Weighted by Mass		
Scenario	Stratosphere	Troposphere	Stratosphere	Troposphere	"Tropopause"[a]
S4	0.766 (1.31)	0.691 (1.45)	220	320	188
S10	0.708 (1.41)	0.679 (1.47)	315	340	285
S4*	0.798 (1.25)	0.749 (1.34)	175	220	140
S10*	0.737 (1.36)	0.736 (1.36)	270	240	235
S3	0.790 (1.27)	0.733 (1.36)	180	245	152
S5	0.736 (1.36)	0.729 (1.37)	265	250	236
S8	0.736 (1.36)	0.697 (1.43)	265	305	236
S8a	0.755 (1.32)	0.722 (1.39)	235	260	205

[a]For comparison to previous box model studies, $\delta D_{h\nu}$ for the "tropopause" was calculated using $\alpha'_{stratosphere}$ (from column 2) and assuming δD-CH_4 = −90‰.

1-D model capable of taking into account the absolute and relative rates of CH_4 and CH_2O oxidation and of CH_2O photolysis to the molecular and radical channels, as well as the rates for the corresponding isotopomers, and how they change with altitude.

3.3. Comparing Stratospheric and Tropospheric Averages for $\alpha'_{CH4\rightarrow H2}$ and $\delta D_{h\nu}$

[46] In order to more broadly assess the implications of the latitude and altitude dependence of $\alpha'_{CH4\rightarrow H2}$ and $\delta D_{h\nu}$ found in this study for using stratospheric observations of δD-H_2 to constrain a global value for $\delta D_{h\nu}$ in the troposphere, as has been done in previous work, stratospheric and tropospheric averages for $\alpha'_{CH4\rightarrow H2}$ and $\delta D_{h\nu}$ were calculated as outlined in section 2.8. The sensitivity of stratospheric and tropospheric mass-weighted annual averages for $\alpha'_{CH4\rightarrow H2}$ and $\delta D_{h\nu}$ to the various IEs we have included in different scenarios is shown in Table 7. We note that averages weighted by CH_4 oxidation rate (not shown) are almost identical to those weighted by mass in the troposphere (since the altitude profiles for mass and CH_4 oxidation rate are proportional), while those in the stratosphere are greatly skewed to the generally smaller values for $\alpha'_{CH4\rightarrow H2}$ and significantly larger values for $\delta D_{h\nu}$ found between 35 and 45 km, where CH_4 oxidation rates are largest.

[47] For the scenarios that happened to best match the ER-2 observations and that yielded very similar δD-H_2:CH_4 relationships (S4, S10, S4*, S10*), mass-weighted averages for stratospheric $\alpha'_{CH4\rightarrow H2}$ range from 0.798 to 0.708 while those for $\delta D_{h\nu}$ range from 175 to 315‰, respectively. The large ranges result from (1) including or not including CH_2O photolysis IEs (∼100‰ as formulated here) or (2) using the *DeMore* [1993] (S4, S10) or the *Gierczak et al.* [1997] (S4*, S10*) KIE for CH_4 + OH (∼50‰). Similar sensitivities are shown by S3, S5, S8, and S8a, which constitute another set of runs that resulted in similar δD-H_2:CH_4 relationships to one another (although significantly different than the observations). For the troposphere, using the DeMore or the Gierczak et al. KIE for CH_4 + OH results in large differences in predicted $\delta D_{h\nu}$ of ∼100‰. Overall, both the direction and magnitude of the differences between the tropospheric and stratospheric averages for $\alpha'_{CH4\rightarrow H2}$ and $\delta D_{h\nu}$ depend on scenario and result from the very different trends in $\delta D_{h\nu}$ with altitude among the various scenarios. Interestingly, for all scenarios run, values calculated for the average tropospheric $\alpha'_{CH4\rightarrow H2}$ are always smaller than (or the same magnitude as) those for the average stratospheric $\alpha'_{CH4\rightarrow H2.}$ While this result may not be robust given the large uncertainties in the underlying isotope effects and their sensitivities to altitude and latitude, it is in contrast to the extrapolation by *Rhee et al.* [2006b] of box model results for stratospheric $\alpha'_{CH4\rightarrow H2}$ to the troposphere in which a value for tropospheric $\alpha'_{CH4\rightarrow H2}$ was derived that was larger than their stratospheric value. Their conclusion, however, is essentially driven by their estimate of the ratio of effective fractionation factors for CH_4 + oxidants in the stratosphere (determined from their stratospheric δD-CH_4 observations) versus the troposphere (based on tropospheric averages of 2-D model results for CH_4 oxidation rates and using the *Gierczak et al.* [1997] CH_4 + OH KIE for an assumed tropospheric average temperature of 277K) since (1) their value for the ratio of the average CH_2O oxidation KIEs for the stratosphere versus the troposphere is relatively close to 1 (=1.0267), (2) they assumed that the ratio of fractionation factors for CH_2O photolysis to the molecular channel for the stratosphere versus the troposphere is 1, and (3) they implicitly assumed (by ignoring it) that the ratio of radical channel isotope effects for the stratosphere versus troposphere is 1. Furthermore, they also assumed that the overall fractionation factor $\alpha'_{CH4\rightarrow H2}$ for both the stratosphere and troposphere can be approximated as the product of the fractionation factors for each category of isotope effect weighted by the chemical rate for that process averaged over the entire troposphere or stratosphere. However, the average of a product does not equal the product of the averages if the factors of the product are not independent and, indeed, our full 2-D model results for $\alpha'_{CH4\rightarrow H2}$ and $\delta D_{h\nu}$ for various scenarios shown in Figures 6–9 and our discussion above show that the effects of IEs for CH_2O photolysis on $\alpha'_{CH4\rightarrow H2}$ and $\delta D_{h\nu}$ are not separable from changes in the absolute and relative rates of CH_2O photolysis to the molecular and radical channel throughout the atmosphere nor from the CH_4 and CH_2O oxidation rates and their KIEs and result in a wide variation in possible values for $\alpha'_{CH4\rightarrow H2}$ and $\delta D_{h\nu}$ as a function of latitude and altitude even when the photolysis isotope effects themselves remain constant. More specifically, on the basis of our sensitivity studies here, it is not likely that the ratios of the CH_2O photolysis isotope effects for the stratosphere and troposphere equal 1 nor that the other ratios of KIEs for the stratosphere versus the troposphere

(weighted by average reaction rates) can be easily separated into independent average factors. Thus our results suggest that the relatively small error bars given for the *Rhee et al.* [2006b] estimates for $\delta D_{h\nu}$ in the troposphere (see Table 1) are not yet warranted. In summary, we conclude that current estimates for tropospheric $\delta D_{h\nu}$ are likely to be neither accurate nor precise and that reducing the uncertainties requires additional laboratory experiments, theoretical calculations, and/or atmospheric observations, coupled with modeling that can account for the probable latitude and altitude dependences of $\alpha'_{CH4\rightarrow H2}$ and $\delta D_{h\nu}$.

3.4. Measurements and Calculations Needed to Reduce Uncertainties in the H_2 Global Isotope Budget

[48] On the basis of our sensitivity studies discussed here, we conclude that in order to further reduce uncertainties in the magnitude of $\delta D_{h\nu}$ and the global isotope budget of H_2 in general, it is essential to determine or reliably estimate the branching ratios in (R1), (R2), (R3), and (R9), whether through experiments or theoretical calculations, as we have shown that choices for these branching ratios lead to a range of predicted δD-H_2 of as much as 400‰. Because (R2) and (R3) are minor channels in the $CH_4 + O(^1D)$ reaction and appear to affect $\delta D_{h\nu}$ only in the upper stratosphere where $O(^1D)$ concentrations are highest, determination of the branching ratios for (R1) and (R9) should be a priority. Furthermore, theoretical calculations by Espinosa-Garcia suggest that the branching ratio for $CH_3D + OH$ may be temperature-dependent (J. Espinosa-Garcia, Universidad de Extremadura, Badajoz, Spain, personal communication, 2006), which in turn suggests that atmospheric $\delta D_{h\nu}$ values may exhibit even more sensitivity to latitude and altitude than captured by our temperature-independent sensitivity runs here. Hence measurements and/or calculations of these branching ratios as a function of temperature are also needed.

[49] It is also clear from our model results that isotope effects in CH_2O photolysis have a significant impact on $\delta D_{h\nu}$, perhaps an even larger impact than our limited sensitivity studies here demonstrate. Determination of the branching ratios in (R1) and (R9) may allow the current database of stratospheric δD-H_2 measurements to be used to provide additional constraints on the underlying CH_2O isotope effects, while further measurements at Earth's surface of the relative photolysis rates and quantum yields for CH_2O and CHDO and the isotopic composition of H_2 produced, perhaps combined with 2-D modeling that includes H_2 and HD surface source and sink fluxes rather than the static surface boundary conditions here, may provide confidence in the current surface constraints and how to extrapolate them to higher altitudes. Our sensitivity study here, however, shows that much uncertainty could be unambiguously resolved if the CHDO absorption cross sections and the molecular and radical channel quantum yields for CHDO photolysis can be accurately measured as a function of wavelength. Temperature and pressure effects on these variables may also need to be taken into account.

[50] Given the especially strong sensitivity of $\delta D_{h\nu}$ in the troposphere to the magnitude and temperature dependence of the $CH_4 + OH$ KIE, further investigation of discrepancies between laboratory KIEs (e.g., *DeMore* [1993] versus *Gierczak et al.* [1997]), stratospheric δD-CH_4 measurements [e.g., *Rice et al.*, 2003; *Rhee et al.*, 2006b], and model simulations [e.g., *McCarthy et al.*, 2003; *Wang et al.*, 2002] are warranted in order to determine the best value for the $CH_4 + OH$ KIE to use for tropospheric and stratospheric applications.

[51] While KIEs for the H_2 and CH_2O oxidation reactions have been measured, studies that could reduce uncertainties in these KIEs would also be valuable in further reducing uncertainties in $\delta D_{h\nu}$. The KIEs for reaction of CH_2O with OH, Cl and Br are now relatively well constrained at room temperature, but an investigation of their temperature and pressure dependence, especially for the OH KIE since OH is the primary oxidant in the troposphere, would aid in further constraining estimates of $\delta D_{h\nu}$. Another determination of the KIE for $CH_2O + O(^3P)$ would also be valuable.

[52] In addition to determination of the isotope effects and branching ratios that determine δD-H_2 and $\delta D_{h\nu}$, direct measurements of atmospheric δD-CH_2O would provide a valuable constraint on values for $\delta D_{h\nu}$, even if such measurements were only possible at first in limited regions of the atmosphere. If values for δD-CH_2O in the atmosphere were known, important constraints on the branching ratios for (R1), (R2), (R3), and (R9) could be obtained. In principle, sufficient knowledge of atmospheric δD-CH_2O might even eliminate the need to know branching ratios in order to predict $\delta D_{h\nu}$, although knowledge of the isotope effects in CH_2O photolysis would still be necessary. We caution, however, that our model results (depending on scenario) suggest that there are large variations in δD-CH_2O with respect to latitude and altitude in the troposphere.

[53] Additional measurements of stratospheric δD-H_2 would also be useful, as well as further investigation of the differences between the δD-H_2:CH_4 relationships measured by *Rahn et al.* [2003] and *Röckmann et al.* [2003]. Laboratory intercomparisons of H_2 isotope measurements will help to determine if the observed measurement differences are primarily analytical or represent real stratospheric variability (e.g., influenced more than expected by mesosphere-to-stratosphere transport based on sensitivity runs performed here), while additional δD-H_2 measurements that expand the current altitude and meridional coverage will provide additional constraints for future modeling efforts.

[54] Finally, we note that our modeled values for $\delta D_{h\nu}$ correspond to the isotopic composition of H_2 produced from the oxidation of CH_4 only. Yet, in the troposphere, it is estimated that ~35% of the photochemical oxidation source of H_2 is derived from NMHCs (see Table 1), and, thus, quantifying the isotopic composition of H_2 produced by NMHC oxidation is likely to be a required component of an accurate H_2 isotope budget [*Gerst and Quay*, 2001]. For some NMHCs, oxidation KIEs have been reported [see, e.g., *Droege and Tully*, 1986, and references therein], and it reasonable to expect that, in general, KIEs for NMHC oxidation will result in lighter values of δD-H_2 and $\delta D_{h\nu}$ in the troposphere than in their absence, similar to the effect of the KIEs for CH_4 oxidation on δD-H_2 and $\delta D_{h\nu}$ shown here. Predicting the isotopic composition of H_2 produced from NMHC oxidation and whether it might be isotopically lighter or heavier than H_2 produced from CH_4 oxidation, however, requires not only knowledge of the H/D KIEs for

NMHC oxidation but also of the branching ratios for H versus D abstraction as NMHCs are oxidized (analogous to branching ratios for CH_4 oxidation (R1)–(R3) and (R9)) and the isotopic compositions of the NMHCs. These requirements mean that much of the fundamental chemical and isotopic data needed for modeling $\delta D_{h\nu}$ of H_2 produced from NMHC oxidation are still lacking.

4. Conclusions

[55] We have used LOTUS, a 2-D chemical-radiative-transport model, to investigate the sensitivity of the isotopic composition of stratospheric H_2 (δD-H_2) and the isotopic composition of H_2 produced from CH_4 oxidation ($\delta D_{h\nu}$) to known and unknown isotope effects in the elementary steps of the photochemical production and destruction of H_2, including KIEs for the reactions of CH_4 with various oxidants, branching ratios for D versus H atom abstraction in the oxidation of CH_3D to HD and H_2, kinetic isotope effects (KIEs) in the oxidation of formaldehyde, possible IEs in formaldehyde photolysis, and KIEs for the oxidation of H_2.

[56] Consistent with previous box model analyses [*Rahn et al.*, 2003; *Röckmann et al.*, 2003; *Rhee et al.*, 2006b], our model results show that approximately 60% of the deuterium enrichment in H_2 over the range of ER-2 observations is controlled by KIEs in the oxidation of H_2, with the remainder determined by the composite of isotope effects in the CH_4-to-H_2 oxidation pathway (i.e., the fractionation factor $\alpha'_{CH4\rightarrow H2}$). However, by explicitly including the elementary reaction steps and their corresponding known or hypothetical isotope effects, our sensitivity runs suggest that a potentially large range of plausible values for the CH_3D oxidation branching ratios and CH_2O photolysis isotope effects, the two categories of isotope effects that are currently the least constrained by measurements and theory, can yield model results for stratospheric δD-H_2 that are consistent with stratospheric observations yet at the same time yielding quite different values for $\alpha_{CH4\rightarrow H2}$ and $\delta D_{h\nu}$ in the troposphere. Furthermore, our 2-D results demonstrate that even for a single model scenario (i.e., for a given set of isotope effects) there are significant variations in $\alpha_{CH4\rightarrow H2}$ and $\delta D_{h\nu}$ with respect to altitude and latitude throughout the atmosphere, driven largely by the temperature dependence of the CH_4 + OH KIE, the changing absolute abundances and relative fractions of the CH_4 and CH_2O oxidant radicals, and a complex (and inseparable) interplay between the relative and absolute rates of CH_2O oxidation, CH_2O photolysis to the molecular and radical channels, and the relative magnitudes of the photolysis isotope effects which play out differently in different regions of the atmosphere, making it difficult to predict how $\alpha_{CH4\rightarrow H2}$ and $\delta D_{h\nu}$ will vary in different regions of the atmosphere without at least a 1-D model. Thus, until additional laboratory and atmospheric observations and/or theoretical calculations become available to better constrain the CH_3D oxidation branching ratios, CH_2O photolysis isotope effects, or both, we conclude that estimation of $\alpha_{CH4\rightarrow H2}$ and $\delta D_{h\nu}$ values for the troposphere based on values for the stratosphere determined by good agreement with stratospheric observations (whether overall $\alpha_{CH4\rightarrow H2}$ values as in the works by *Rahn et al.* [2003] or *Röckmann et al.* [2003] or $\alpha_{CH4\rightarrow H2}$ values partitioned into fractionation factors for oxidation, branching, and photolysis reactions then "corrected" for average tropospheric conditions as in *Rhee et al.* [2006b]) is not reliable and caution that recent estimates for tropospheric $\delta D_{h\nu}$ may have much larger uncertainties than the reported error bars.

[57] We have also used the 2-D model sensitivities to identify the experimental, theoretical, modeling, and field work most needed to reduce uncertainties in $\delta D_{h\nu}$ and conclude that determining the unknown branching ratios in the CH_3D oxidation pathway, the absorption cross sections for CHDO, and the molecular and radical channel quantum yields for CHDO photolysis as a function of wavelength should be top priorities. Further reducing uncertainties in the measured KIEs for CH_4 and CH_2O oxidation and their temperature dependences, observations of the isotopic composition of atmospheric formaldehyde, and laboratory intercomparisons of δD-H_2 measurements should also serve to better constrain $\delta D_{h\nu}$ and the molecular level isotope effects that determine it. Improving the accuracy of the magnitude of $\delta D_{h\nu}$ will, in turn, better constrain the global H_2 isotope budget in general, while a molecular level understanding of the isotope effects, once demonstrated in 2-D models compared against a range of atmospheric observations, will allow incorporation of these isotope effects into 3-D models used to gain a mechanistic understanding of the current H_2 budget and to predict the potential environmental impacts of increased H_2 emissions that are likely to accompany a shift to fuel cell technologies.

[58] **Acknowledgments.** We gratefully acknowledge support for this research from the University of California Energy Institute (UCEI); the NASA Atmospheric Chemistry, Modeling and Analysis Program; the David and Lucile Packard Foundation; the Camille Dreyfus Teacher-Scholar Award; and an NSF Predoctoral Fellowship for K.A.M. We thank Dale Hurst and Jim Elkins for providing the H_2 and CH_4 mixing ratio measurements, Thomas Röckmann for providing the balloon δD-H_2 isotope observations, Claus Nielsen for providing unpublished relative formaldehyde photolysis rates, Joaquin Espinosa-Garcia for providing unpublished values for the CH_3D + OH branching ratio, and three anonymous reviewers for insightful comments and suggestions. This work was partially performed under the auspices of the U.S. Department of Energy by University of California, Lawrence Livermore National Laboratory under contract W-7405-Eng-48.

References

Andrews, A. E., K. A. Boering, S. C. Wofsy, B. C. Daube, D. B. Jones, S. Alex, M. Loewenstein, J. R. Podolske, and S. E. Strahan (2001), Empirical age spectra for the midlatitude lower stratosphere from in situ observations of stratospheric CO_2: Quantitative evidence for a subtropical "barrier" to horizontal transport, *J. Geophys. Res.*, *106*, 10,257–10,274.

Bigeleisen, J., F. S. Klein, R. E. Weston, and M. Wolfsberg (1959), Deuterium isotope effect in the reaction of hydrogen molecules with chlorine atoms and the potential energy of the H_2Cl transition complex, *J. Chem. Phys.*, *30*, 1340–1351.

Cantrell, C. A., J. A. Davidson, A. H. McDaniel, R. E. Shetter, and J. G. Calvert (1990), Temperature-dependent formaldehyde cross-sections in the near-ultraviolet spectral region, *J. Phys. Chem.*, *94*, 3902–3908.

Crounse, J. D., T. Rahn, P. O. Wennberg, and J. Eiler (2003), Isotopic composition of molecular hydrogen formed from the photolysis of formaldehyde in sunlight, *Eos Trans. AGU*, *84*(46), Fall Meet. Suppl., Abstract A52A-0771.

D'Anna, B., V. Bakken, J. A. Beukes, C. J. Nielsen, K. Brudnik, and J. T. Jodkowski (2003), Experimental and theoretical studies of gas phase NO_3 and OH radical reactions with formaldehyde, acetaldehyde and their isotopomers, *Phys. Chem. Chem. Phys.*, *5*, 1790–1805.

DeMore, W. B. (1993), Rate-constant ratio for the reactions of OH with CH_3D and CH_4, *J. Phys. Chem.*, *97*, 8564–8566.

Droege, A. T., and F. P. Tully (1986), Hydrogen-atom abstraction from alkanes by OH. 5. n-butane, *J. Phys. Chem.*, *90*, 5937–5941.

Ehhalt, D. H., J. A. Davidson, C. A. Cantrell, I. Friedman, and S. Tyler (1989), The kinetic isotope effect in the reaction of H_2 with OH, *J. Geophys. Res.*, *94*, 9831–9836.

Elkins, J. W., et al. (1996), Airborne gas chromatograph for in situ measurements of long-lived species in the upper troposphere and lower stratosphere, *Geophys. Res. Lett.*, *23*, 347–350.

Feilberg, K. L., M. S. Johnson, and C. J. Nielsen (2004), Relative reaction rates of HCHO, HCDO, DCDO, $H^{13}CHO$, and $HCH^{18}O$ with OH, Cl, Br, and NO_3 radicals, *J. Phys. Chem. A*, *108*, 7393–7398.

Gerst, S., and P. Quay (2000), The deuterium content of atmospheric molecular hydrogen: Method and initial measurements, *J. Geophys. Res.*, *105*, 26,433–26,445.

Gerst, S., and P. Quay (2001), Deuterium component of the global molecular hydrogen cycle, *J. Geophys. Res.*, *106*, 5021–5031.

Gierczak, T., R. K. Talukdar, S. C. Herndon, G. L. Vaghjiani, and A. R. Ravishankara (1997), Rate coefficients for the reactions of hydroxyl radicals with methane and deuterated methanes, *J. Phys. Chem. A*, *101*, 3125–3134.

Hauglustaine, D. A., and D. H. Ehhalt (2002), A three-dimensional model of molecular hydrogen in the troposphere, *J. Geophys. Res.*, *107*(D17), 4330, doi:10.1029/2001JD001156.

Herman, R. L., et al. (2002), Hydration, dehydration, and the total hydrogen budget of the 1999/2000 winter Arctic stratosphere, *J. Geophys. Res.*, *107*, 8320, doi:10.1029/2001JD001257 [printed *108*(D5), 2003].

Khalil, M. A. K., and R. A. Rasmussen (1990), Global increase of atmospheric molecular-hydrogen, *Nature*, *347*, 743–745.

Kinnison, D. E., K. E. Grant, P. S. Connell, D. A. Rotman, and D. J. Wuebbles (1994), The chemical and radiative effects of the Mount Pinatubo eruption, *J. Geophys. Res.*, *99*, 25,705–25,731.

Liang, M. C., G. A. Blake, and Y. L. Yung (2004), A semianalytic model for photo-induced isotopic fractionation in simple molecules, *J. Geophys. Res.*, *109*, D10308, doi:10.1029/2004JD004539.

McCarthy, M. C., P. Connell, and K. A. Boering (2001), Isotopic fractionation of methane in the stratosphere and its effect on free tropospheric isotopic compositions, *Geophys. Res. Lett.*, *28*, 3657–3660.

McCarthy, M. C., K. A. Boering, A. L. Rice, S. C. Tyler, P. Connell, and E. Atlas (2003), Carbon and hydrogen isotopic compositions of stratospheric methane: 2. Two-dimensional model results and implications for kinetic isotope effects, *J. Geophys. Res.*, *108*(D15), 4461, doi:10.1029/2002JD003183.

McCarthy, M. C., K. A. Boering, T. Rahn, J. M. Eiler, A. L. Rice, S. C. Tyler, S. Schauffler, E. Atlas, and D. G. Johnson (2004), The hydrogen isotopic composition of water vapor entering the stratosphere inferred from high precision measurements of δD-CH_4 and δD-H_2, *J. Geophys. Res.*, *109*, D07304, doi:10.1029/2003JD004003.

McQuigg, R. D., and J. G. Calvert (1969), Photodecomposition of CH_2O, CD_2O, CHDO, and CH_2O-CD_2O mixtures at xenon flash lamp intensities, *J. Am. Chem. Soc.*, *91*, 1590–1599.

Miller, W. H. (1979), Tunneling corrections to unimolecular rate constants, with application to formaldehyde, *J. Am. Chem. Soc.*, *101*, 6810–6814.

Moortgat, G. K., W. Seiler, and P. Warneck (1983), Photo-dissociation of HCHO in air—CO and H_2 quantum yields at 220-K and 300-K, *J. Chem. Phys.*, *78*, 1185–1190.

Morris, E. D., and H. Niki (1971), Mass spectrometric study of reaction of hydroxyl radical with formaldehyde, *J. Chem. Phys.*, *55*, 1991–1992.

Nanbu, S., and M. S. Johnson (2004), Analysis of the ultraviolet absorption cross sections of six isotopically substituted nitrous oxide species using 3D wave packet propagation, *J. Phys. Chem. A*, *108*, 8905–8913.

Newman, P., et al. (2002), An overview of the SOLVE-THESEO 2000 campaign, *J. Geophys. Res.*, *107*(D20), 8259, doi:10.1029/2001JD001303.

Niki, H., E. E. Daby, and B. Weinstock (1969), Mass spectrometric study of the kinetics and mechanism of the ethylene-atomic oxygen reaction by the discharge-flow technique at 300°K, paper presented at Twelfth International Symposium on Combustion, Combust. Inst., Pittsburgh, Pa.

Novelli, P. C., P. M. Lang, K. A. Masarie, D. F. Hurst, R. Myers, and J. W. Elkins (1999), Molecular hydrogen in the troposphere: Global distribution and budget, *J. Geophys. Res.*, *104*, 30,427–30,444.

Persky, A., and F. S. Klein (1966), Kinetic isotope effects in reaction between atomic chlorine and molecular hydrogen. Tunnel coefficients of hydrogen atom through an asymmetric potential barrier, *J. Chem. Phys.*, *44*, 3617–3626.

Plumb, R. A., and M. K. W. Ko (1992), Interrelationships between mixing ratios of long lived stratospheric constituents, *J. Geophys. Res.*, *97*, 10,145–10,156.

Plumb, R. A., W. Heres, J. L. Neu, N. M. Mahowald, J. del Corral, G. C. Toon, E. Ray, F. Moore, and A. E. Andrews (2003), Global tracer modeling during SOLVE: High-latitude descent and mixing, *J. Geophys. Res.*, *108*(D5), 8309, doi:10.1029/2001JD001023.

Prakash, M. K., J. D. Weibel, and R. A. Marcus (2005), Isotopomer fractionation in the UV photolysis of N_2O: Comparison of theory and experiment, *J. Geophys. Res.*, *110*, D21315, doi:10.1029/2005JD006127.

Prather, M. J. (2003), An environmental experiment with H_2?, *Science*, *302*(5645), 581–582.

Rahn, T., N. Kitchen, and J. Eiler (2002), D/H ratios of atmospheric H_2 in urban air: Results using new methods for analysis of nano-molar H_2 samples, *Geochim. Cosmochim. Acta*, *66*, 2475–2481.

Rahn, T., J. M. Eiler, K. A. Boering, P. O. Wennberg, M. C. McCarthy, S. Tyler, S. Schauffler, S. Donnelly, and E. Atlas (2003), Extreme deuterium enrichment in stratospheric hydrogen and the global atmospheric budget of H_2, *Nature*, *424*, 918–921.

Rhee, T. S., T. Röckmann, M. Brass, A. Engel, and C. A. M. Brenninkmeijer (2004), The stable isotope composition of stratospheric and mesospheric H_2, *Eos Trans. AGU*, *84*(47), Fall Meet. Suppl., Abstract A23E-06.

Rhee, T. S., C. A. M. Brenninkmeijer, and T. Röckmann (2006a), The overwhelming role of soils in the global atmospheric hydrogen cycle, *Atmos. Chem. Phys.*, *6*, 1611–1625.

Rhee, T. S., C. A. M. Brenninkmeijer, M. Braß, and C. Brühl (2006b), Isotopic composition of H_2 from CH_4 oxidation in the stratosphere and troposphere, *J. Geophys. Res.*, *111*, D23303, doi:10.1029/2005JD006760.

Rice, A. L., S. C. Tyler, M. C. McCarthy, K. A. Boering, and E. Atlas (2003), Carbon and hydrogen isotopic compositions of stratospheric methane: 1. High-precision observations from the NASA ER-2 aircraft, *J. Geophys. Res.*, *108*(D15), 4460, doi:10.1029/2002JD003042.

Röckmann, T., T. S. Rhee, and A. Engel (2003), Heavy hydrogen in the stratosphere, *Atmos. Chem. Phys.*, *3*, 2015–2023.

Romashkin, P. A., D. F. Hurst, J. W. Elkins, G. S. Dutton, D. W. Fahey, R. E. Dunn, F. L. Moore, R. C. Myers, and B. D. Hall (2001), In situ measurements of long-lived trace gases in the lower stratosphere by gas chromatography, *J. Atmos. Oceanic Technol.*, *18*, 1195–1204.

Sander, S. P., et al. (2006), Chemical kinetics and photochemical data for use in atmospheric studies, evaluation number 15, *JPL Publ.*, *06-2*, NASA Jet Propul. Lab., Pasadena, Calif.

Sandor, B. J., and R. T. Clancy (2003), HDO in the mesosphere: Observation and modeling of novel isotopic variability, *J. Geophys. Res.*, *108*(D15), 4463, doi:10.1029/2002JD003193.

Saueressig, G., P. Bergamaschi, J. N. Crowley, H. Fischer, and G. W. Harris (1996), D/H kinetic isotope effect in the reaction CH_4 + Cl, *Geophys. Res. Lett.*, *23*, 3619–3622.

Saueressig, G., J. N. Crowley, P. Bergamaschi, C. Bruhl, C. A. M. Brenninkmeijer, and H. Fischer (2001), Carbon 13 and D kinetic isotope effects in the reactions of CH_4 + $O(^1D)$ and OH: New laboratory measurements and their implications for the isotopic composition of stratospheric methane, *J. Geophys. Res.*, *106*, 23,127–23,138.

Schultz, M. G., T. Diehl, G. P. Brasseur, and W. Zittel (2003), Air pollution and climate-forcing impacts of a global hydrogen economy, *Science*, *302*, 624–627.

Simmonds, P. G., R. G. Derwent, S. O'Doherty, D. B. Ryall, L. P. Steele, R. L. Langenfelds, P. Salameh, H. J. Wang, C. H. Dimmer, and L. E. Hudson (2000), Continuous high-frequency observations of hydrogen at the Mace Head baseline atmospheric monitoring station over the 1994–1998 period, *J. Geophys. Res.*, *105*, 12,105–12,121.

Taatjes, C. A. (1999), Infrared frequency-modulation measurements of absolute rate coefficients for Cl + HD → HCl(DCl) + D(H) between 295 and 700 K, *Chem. Phys. Lett.*, *306*, 33–40. (Errata, *Chem. Phys. Lett.*, *380*, 490, 2003.)

Talukdar, R. K., and A. R. Ravishankara (1996), Rate coefficients for O(^{1}D) + H_2, D_2, HD reactions and H atom yield in O(^{1}D) + HD reaction, *Chem. Phys. Lett.*, *253*, 177–183.

Talukdar, R. K., T. Gierczak, L. Goldfarb, Y. Rudich, B. S. M. Rao, and A. R. Ravishankara (1996), Kinetics of hydroxyl radical reactions with isotopically labeled hydrogen, *J. Phys. Chem.*, *100*, 3037–3043.

Tromp, T. K., R. L. Shia, M. Allen, J. M. Eiler, and Y. L. Yung (2003), Potential environmental impact of a hydrogen economy on the stratosphere, *Science*, *300*, 1740–1742.

Tyler, S. C., H. O. Ajie, A. L. Rice, R. J. Cicerone, and E. C. Tuazon (2000), Experimentally determined kinetic isotope effects in the reaction of CH_4 with Cl: Implications for atmospheric CH_4, *Geophys. Res. Lett.*, *27*, 1715–1718.

Wang, J. S., M. B. McElroy, C. M. Spivakovsky, and D. B. A. Jones (2002), On the contribution of anthropogenic Cl to the increase in δ^{13}C of atmo-

spheric methane, *Global Biogeochem. Cycles*, *16*(3), 1047, doi:10.1029/2001GB001572.

Warwick, N. J., S. Bekki, E. G. Nisbet, and J. A. Pyle (2004), Impact of a hydrogen economy on the stratosphere and troposphere studied in a 2-D model, *Geophys. Res. Lett.*, *31*, L05107, doi:10.1029/2003GL019224.

Waugh, D. W., et al. (1997), Mixing of polar vortex air into middle latitudes as revealed by tracer-tracer scatterplots, *J. Geophys. Res.*, *102*, 13,119–13,134.

World Meteorological Organization (1999), Scientific assessment of O_3 depletion: 1998, *Proj. Rep. 44*, U.N. Environ. Programme, Geneva, Switzerland.

Yung, Y. L., and C. E. Miller (1997), Isotopic fractionation of stratospheric nitrous oxide, *Science*, *278*, 1778–1780.

K. A. Boering and K. A. Mar, Department of Chemistry, University of California, Berkeley, CA 94720, USA. (boering@berkeley.edu)

P. Connell, Energy and Environment Directorate, Lawrence Livermore National Laboratory, Livermore, CA 94550, USA.

M. C. McCarthy, Sonoma Technology, Inc., 1360 Redwood Way, Suite C, Petaluma, CA 94954, USA.